Supporting Information for

"Water-wave-induced Ocean-Bottom Seismometer (OBS) noise : theories, observations and potential application"

Chun Zhang, Chao An

Contents

Corresponding author: Chao An, anchao@sjtu.edu.cn

Figure S1

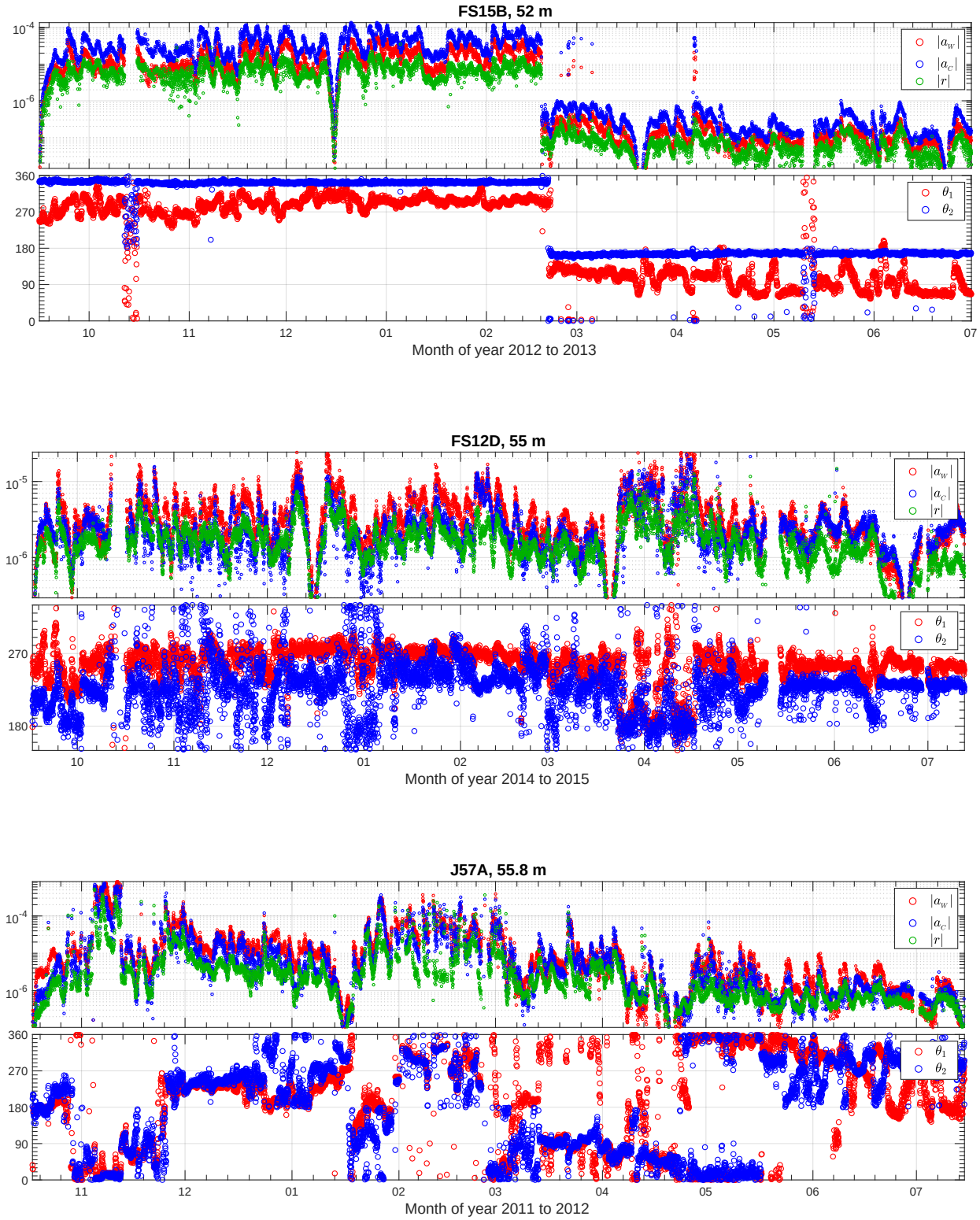
FS15B, 52 m
10^{-4}
10^{-6}
$|a_w|$
$|a_c|$
$|r|$
360
270
180
90
0
θ_1
θ_2
10
11
12
01
02
03
04
05
06
07
Month of year 2012 to 2013
FS12D, 55 m
10^{-5}
10^{-6}
$|a_w|$
$|a_c|$
$|r|$
270
180
θ_1
θ_2
10
11
12
01
02
03
04
05
06
07
Month of year 2014 to 2015
J57A, 55.8 m
10^{-4}
10^{-6}
$|a_w|$
$|a_c|$
$|r|$
360
270
180
90
0
θ_1
θ_2
11
12
01
02
03
04
05
06
07
Month of year 2011 to 2012

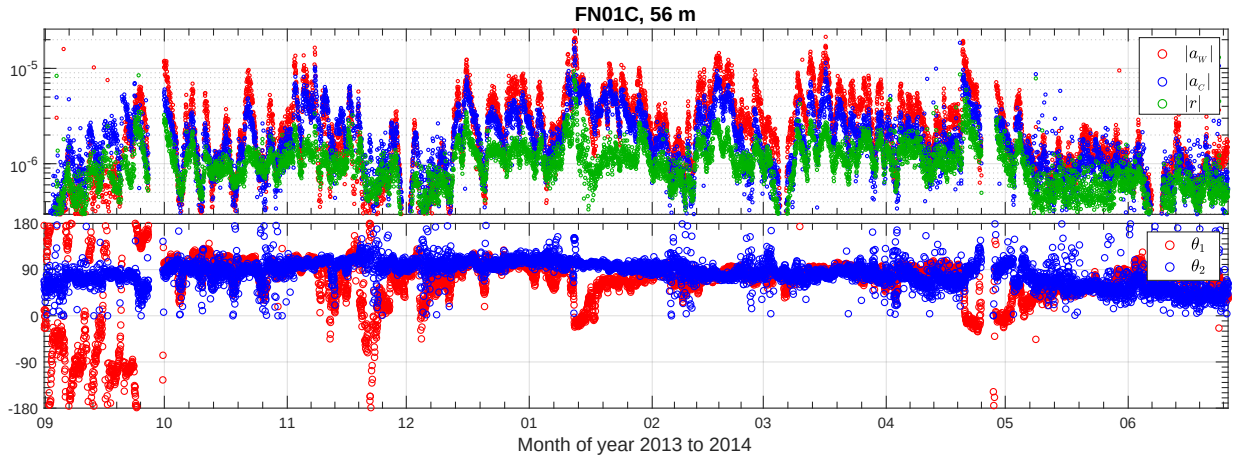
FN01C, 56 m
$|a_w|$
$|a_c|$
$|r|$
θ_1
θ_2
Month of year 2013 to 2014

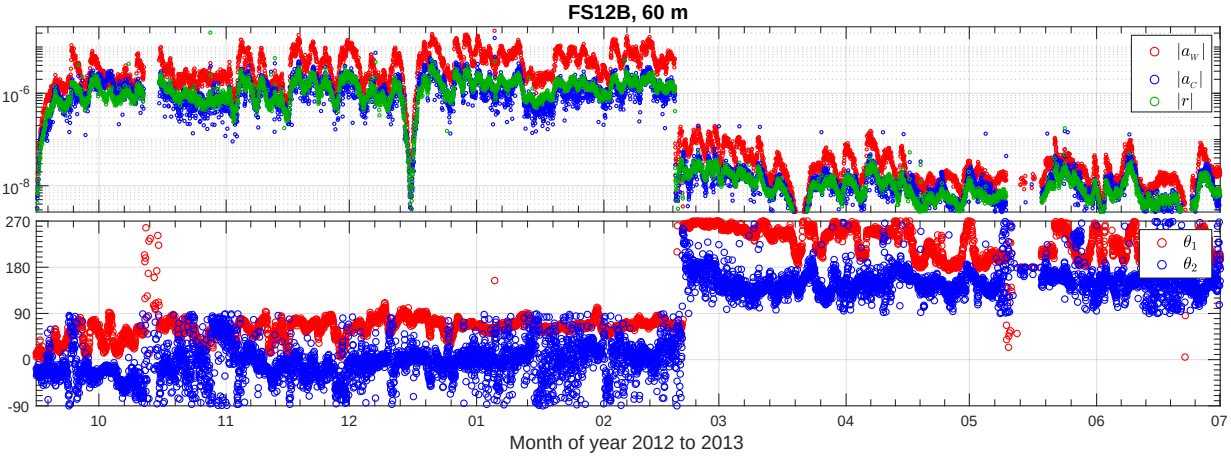
FS12B, 60 m
$|a_w|$
$|a_c|$
$|r|$
θ_1
θ_2
Month of year 2012 to 2013

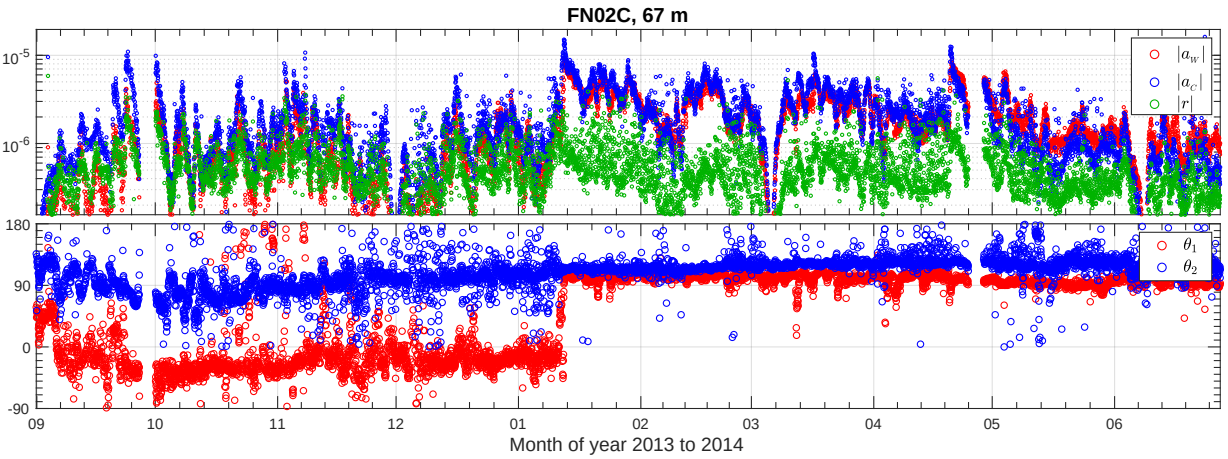
FN02C, 67 m
$|a_w|$
$|a_c|$
$|r|$
θ_1
θ_2
Month of year 2013 to 2014

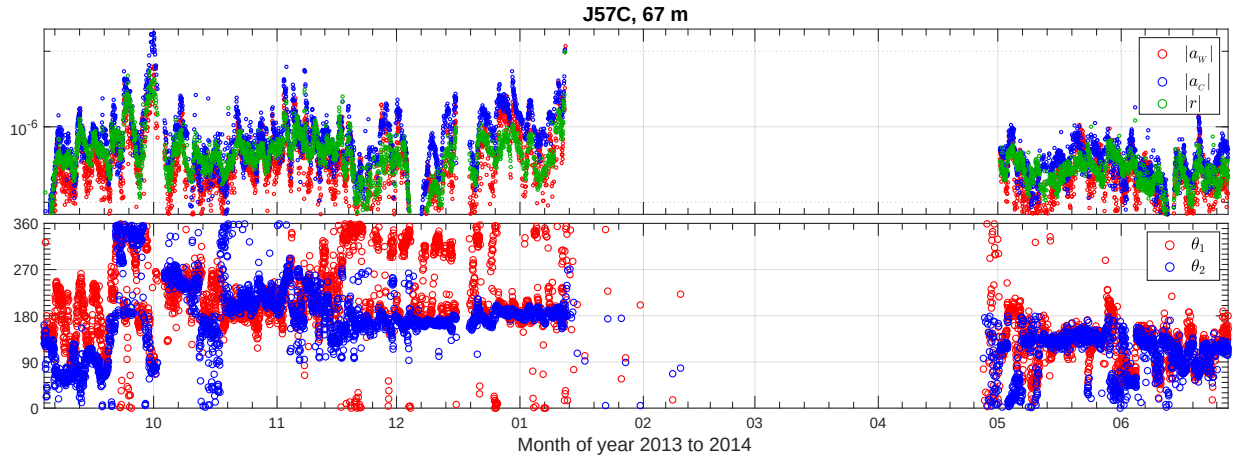
J57C, 67 m
10^{-6}
$|a_w|$
$|a_c|$
$|r|$
360
270
180
90
0
θ_1
θ_2
10
11
12
01
02
03
04
05
06
Month of year 2013 to 2014

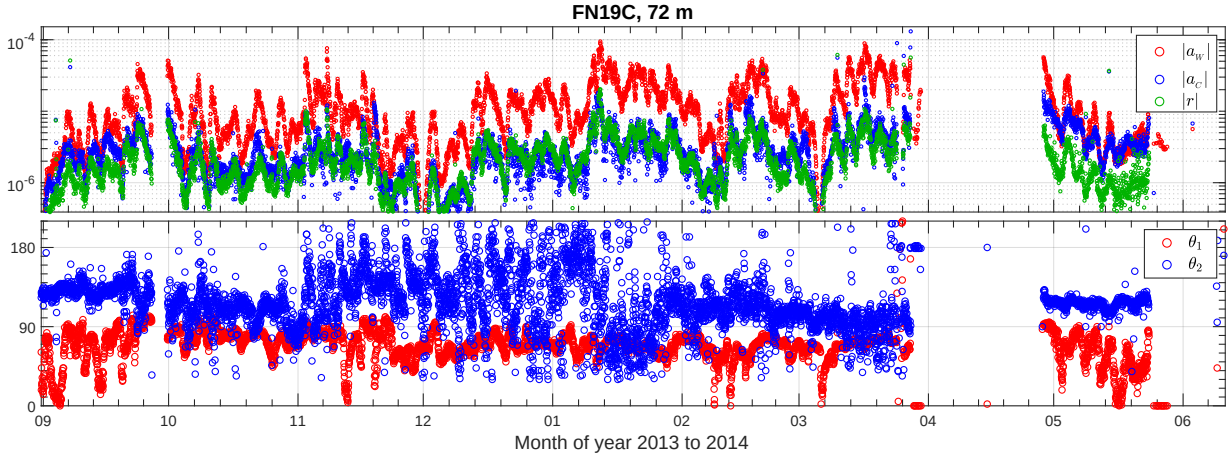
FN19C, 72 m
10^{-4}
10^{-6}
$|a_w|$
$|a_c|$
$|r|$
180
90
0
θ_1
θ_2
09
10
11
12
01
02
03
04
05
06
Month of year 2013 to 2014

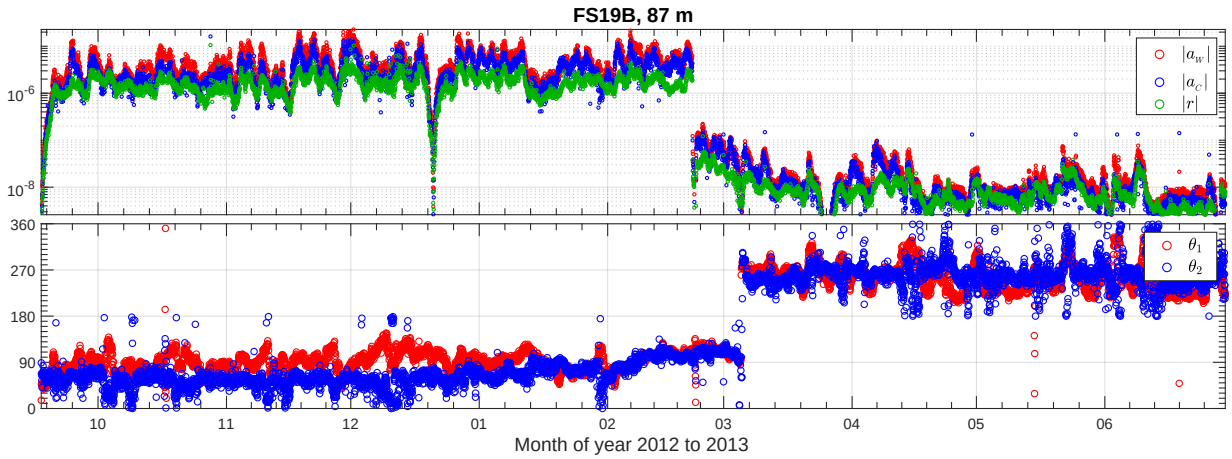
FS19B, 87 m
10^{-6}
10^{-8}
$|a_w|$
$|a_c|$
$|r|$
360
270
180
90
0
θ_1
θ_2
10
11
12
01
02
03
04
05
06
Month of year 2012 to 2013

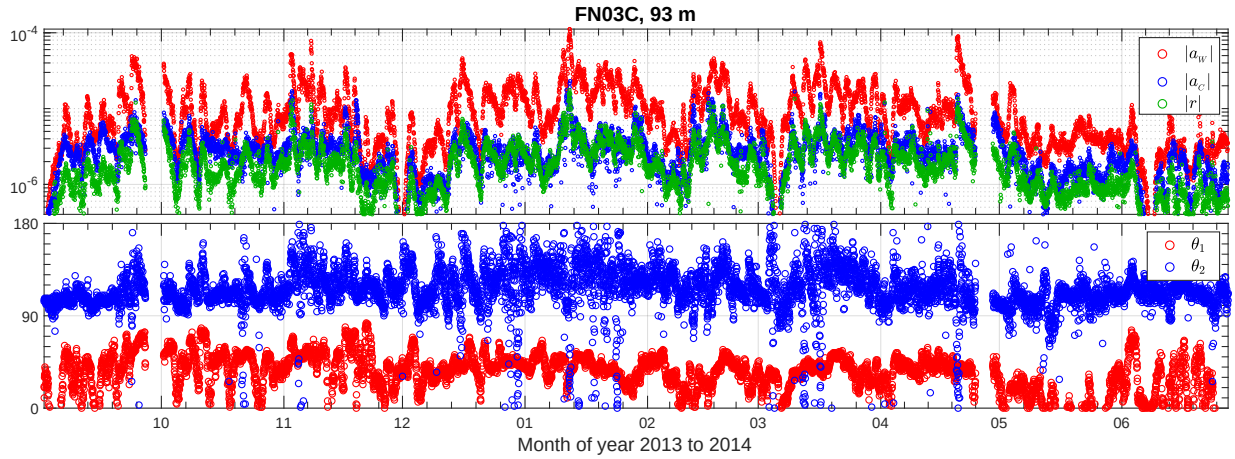
FN03C, 93 m
10^{-4}
10^{-6}
$|a_w|$
$|a_c|$
$|r|$
180
90
0
θ_1
θ_2
10
11
12
01
02
03
04
05
06
Month of year 2013 to 2014

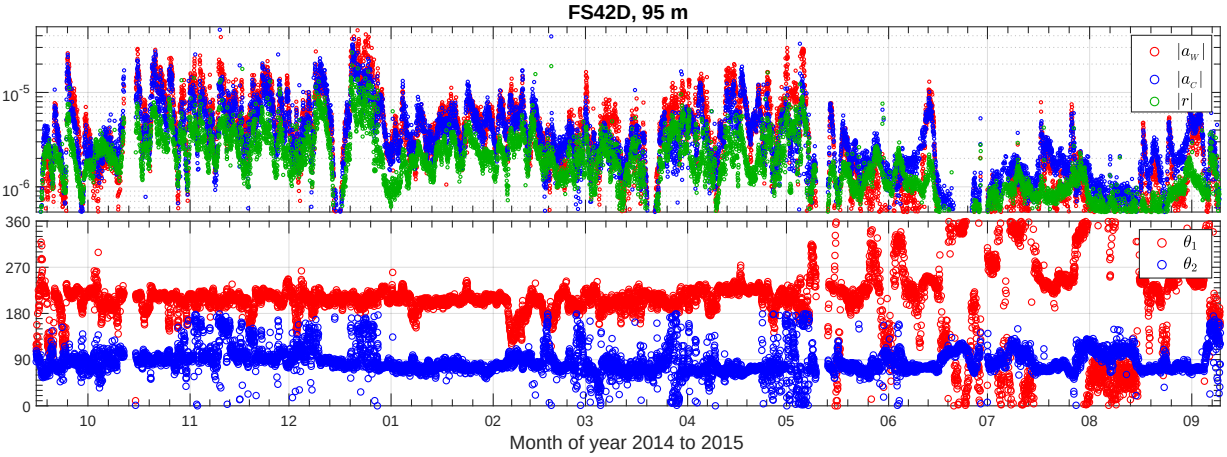
FS42D, 95 m
10^{-5}
10^{-6}
$|a_w|$
$|a_c|$
$|r|$
360
270
180
90
0
θ_1
θ_2
10
11
12
01
02
03
04
05
06
07
08
09
Month of year 2014 to 2015

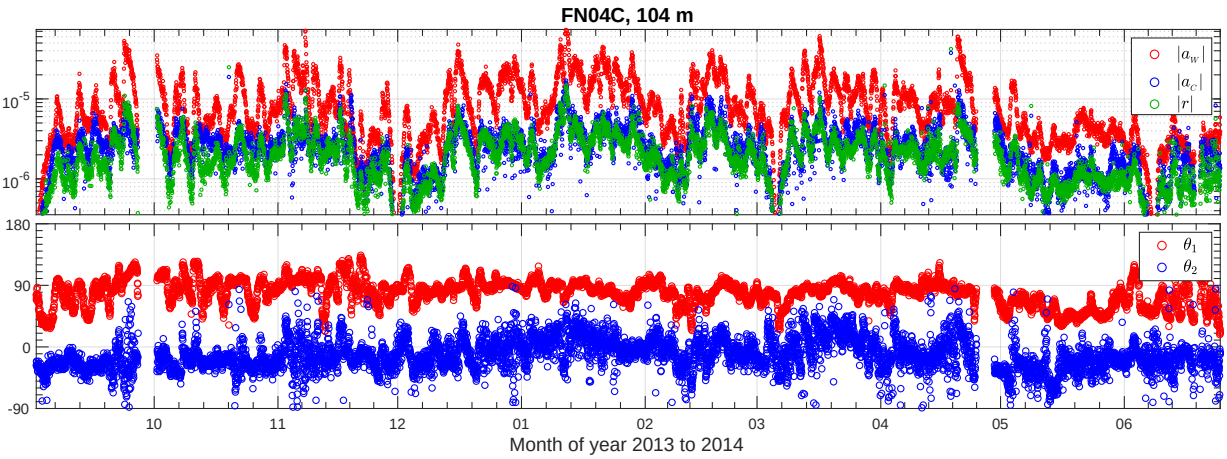
FN04C, 104 m
10^{-5}
10^{-6}
$|a_w|$
$|a_c|$
$|r|$
180
90
0
-90
θ_1
θ_2
10
11
12
01
02
03
04
05
06
Month of year 2013 to 2014

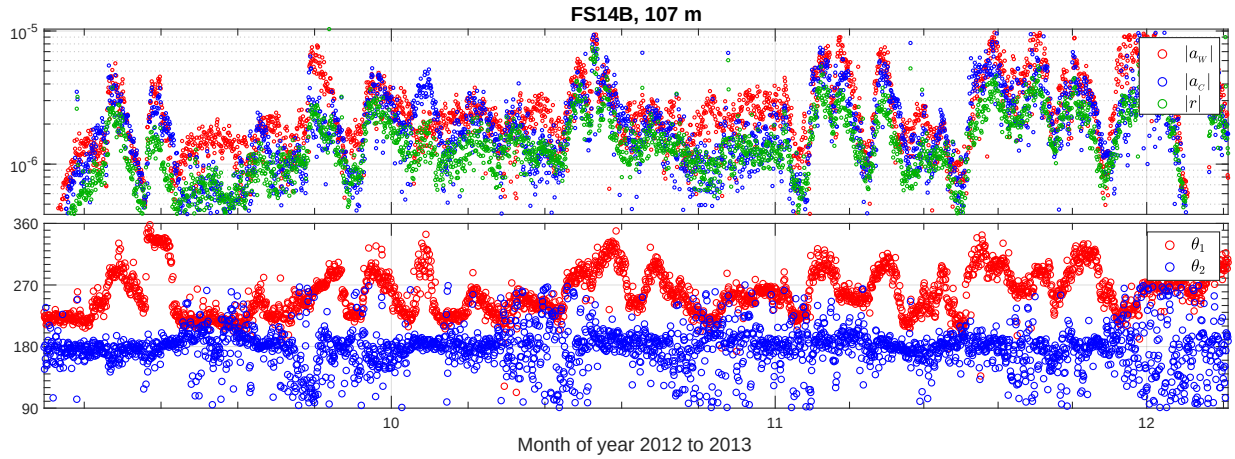
FS14B, 107 m
10^{-5}
10^{-6}
$|a_w|$
$|a_c|$
$|r|$
360
270
180
90
θ_1
θ_2
10
11
12
Month of year 2012 to 2013

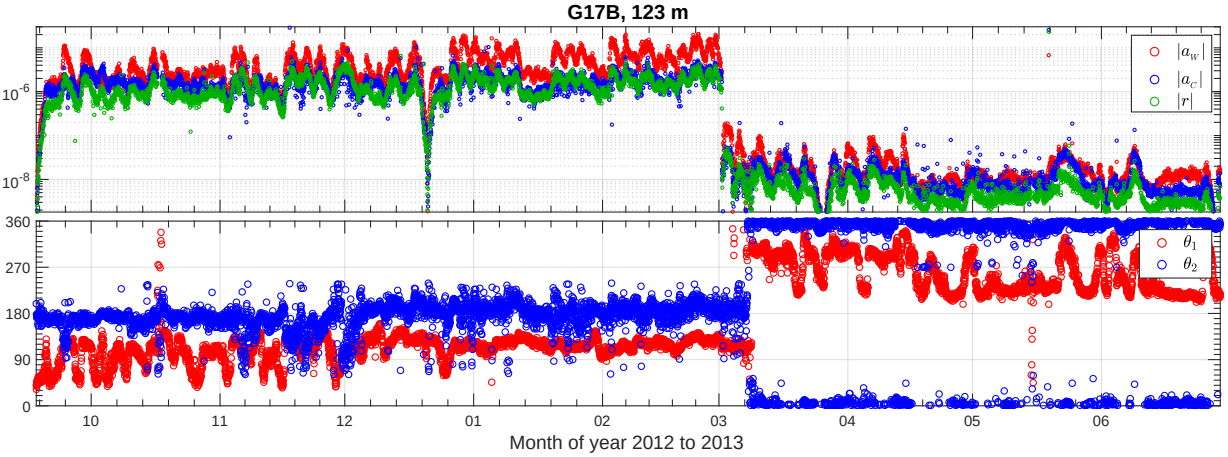
G17B, 123 m
10^{-6}
10^{-8}
$|a_w|$
$|a_c|$
$|r|$
360
270
180
90
0
θ_1
θ_2
10
11
12
01
02
03
04
05
06
Month of year 2012 to 2013

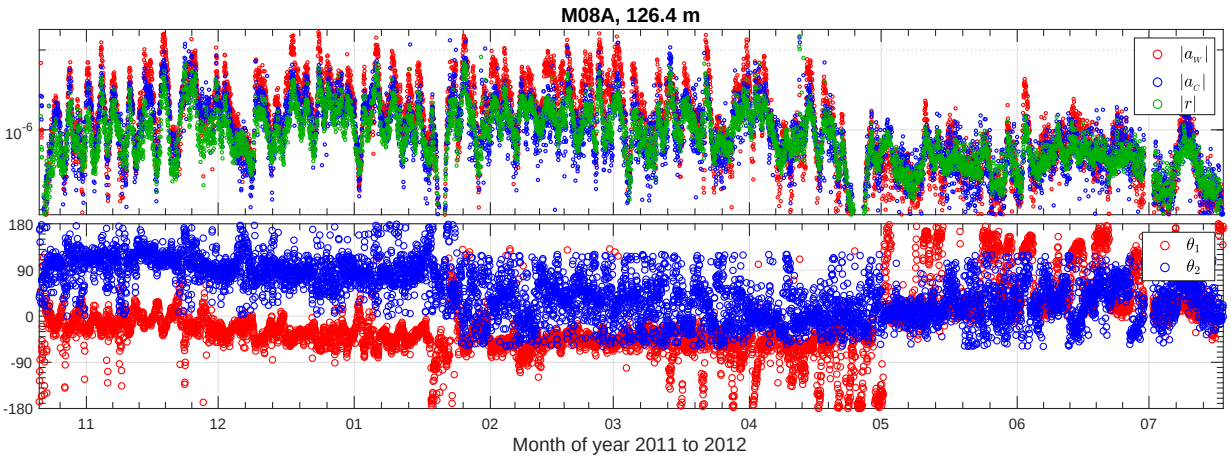
M08A, 126.4 m
10^{-6}
$|a_w|$
$|a_c|$
$|r|$
180
90
0
-90
-180
θ_1
θ_2
11
12
01
02
03
04
05
06
07
Month of year 2011 to 2012

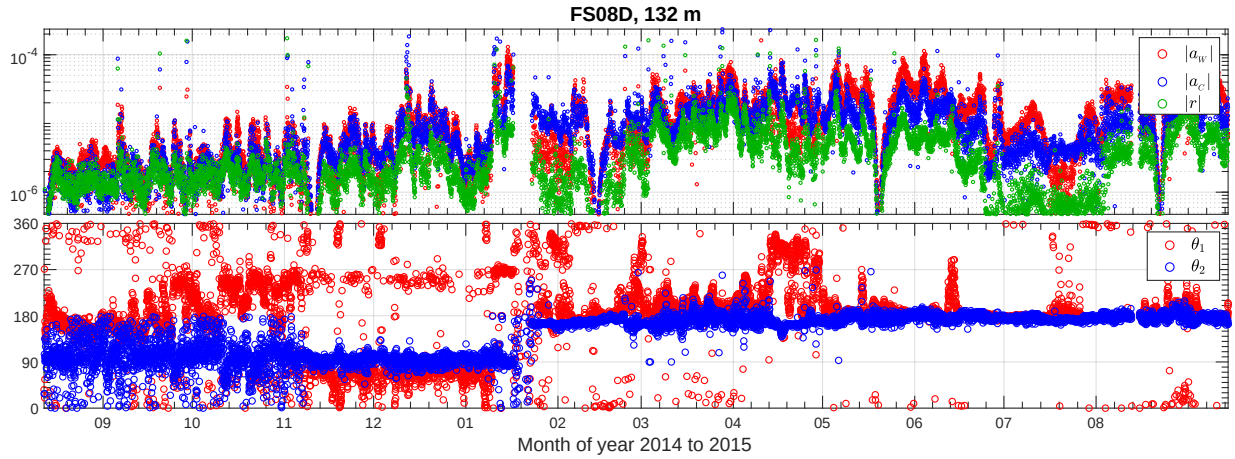
FS08D, 132 m
10^{-4}
10^{-6}
$|a_w|$
$|a_c|$
$|r|$
360
270
180
90
0
θ_1
θ_2
09
10
11
12
01
02
03
04
05
06
07
08
Month of year 2014 to 2015

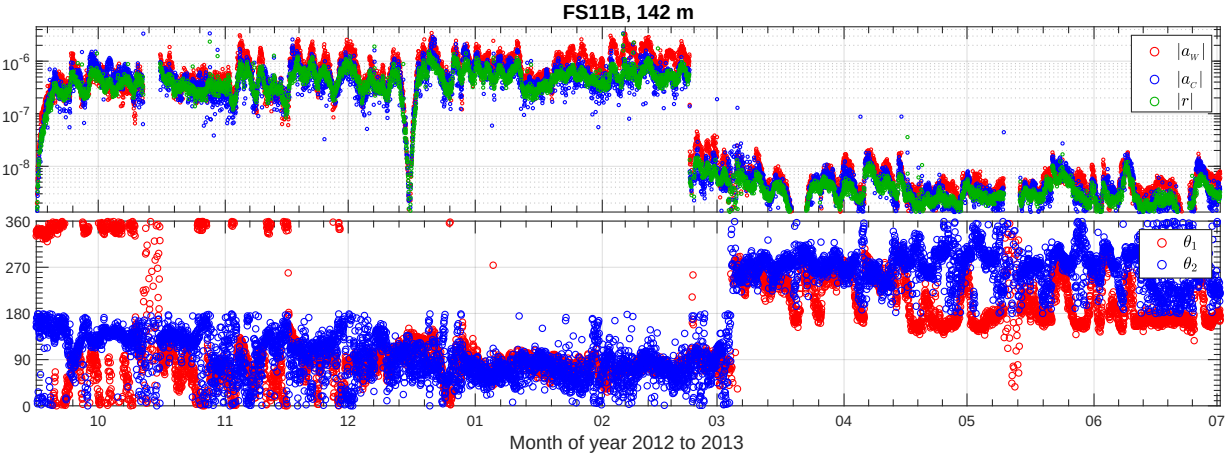
FS11B, 142 m
10^{-6}
10^{-7}
10^{-8}
$|a_w|$
$|a_c|$
$|r|$
360
270
180
90
0
θ_1
θ_2
10
11
12
01
02
03
04
05
06
07
Month of year 2012 to 2013

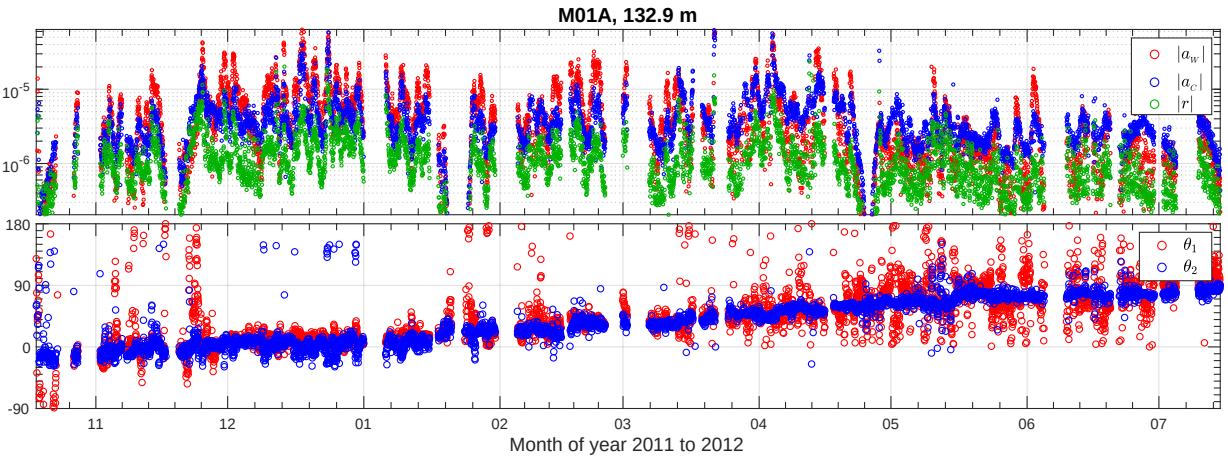
M01A, 132.9 m
10^{-5}
10^{-6}
$|a_w|$
$|a_c|$
$|r|$
180
90
0
-90
θ_1
θ_2
11
12
01
02
03
04
05
06
07
Month of year 2011 to 2012

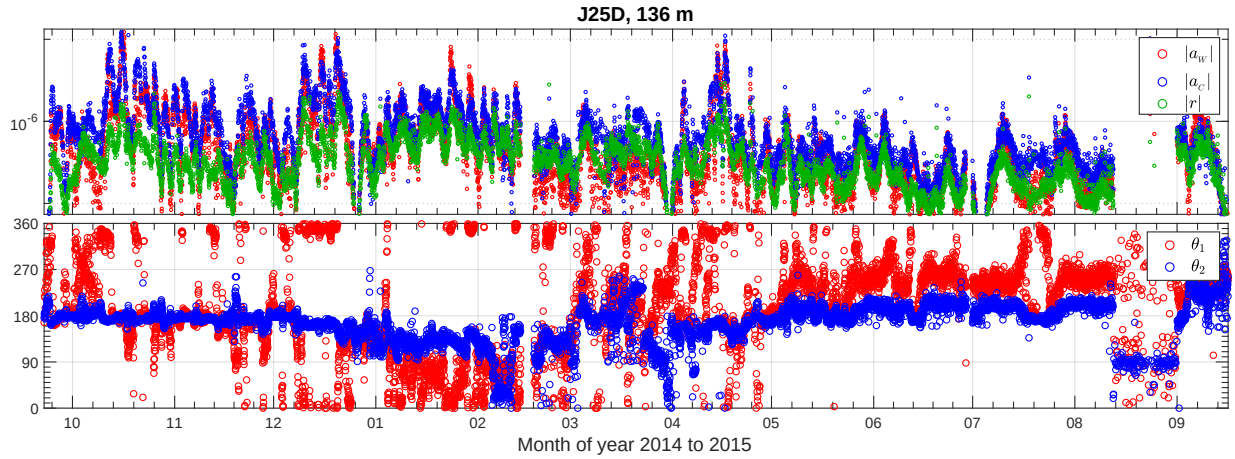
J25D, 136 m
10^{-6}
$|a_w|$
$|a_c|$
$|r|$
360
270
180
90
0
θ_1
θ_2
10
11
12
01
02
03
04
05
06
07
08
09
Month of year 2014 to 2015

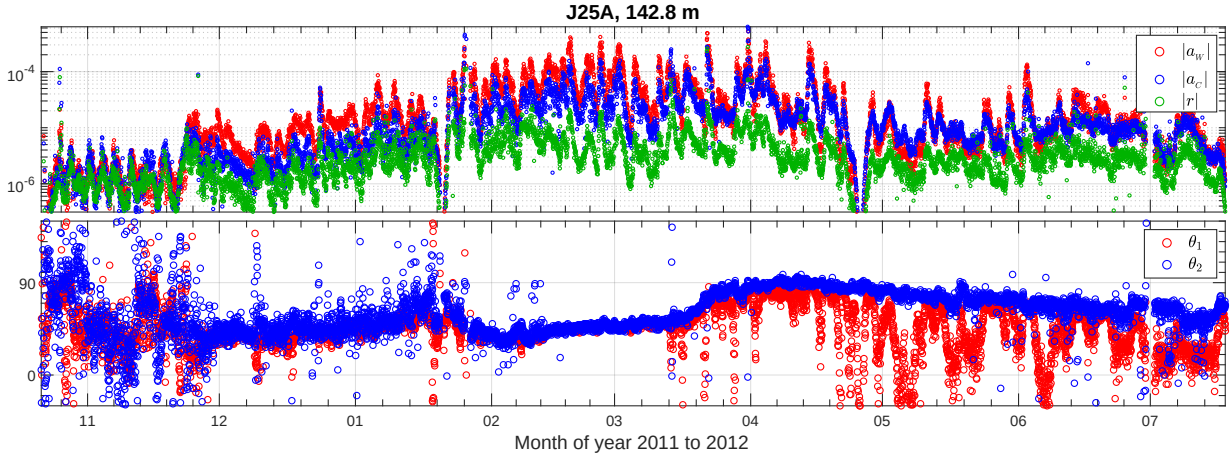
J25A, 142.8 m
10^{-4}
10^{-6}
$|a_w|$
$|a_c|$
$|r|$
90
0
θ_1
θ_2
11
12
01
02
03
04
05
06
07
Month of year 2011 to 2012

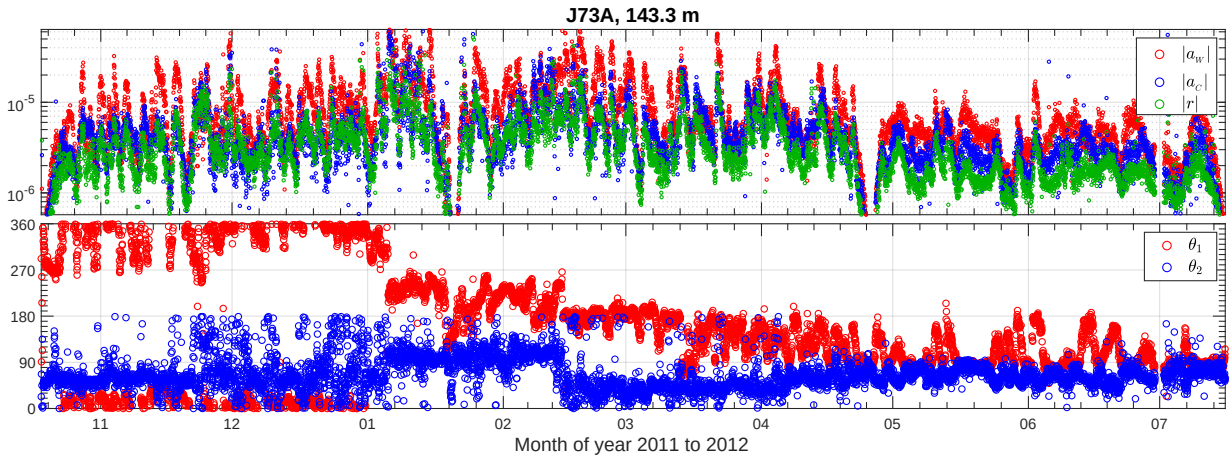
J73A, 143.3 m
10^{-5}
10^{-6}
$|a_w|$
$|a_c|$
$|r|$
360
270
180
90
0
θ_1
θ_2
11
12
01
02
03
04
05
06
07
Month of year 2011 to 2012

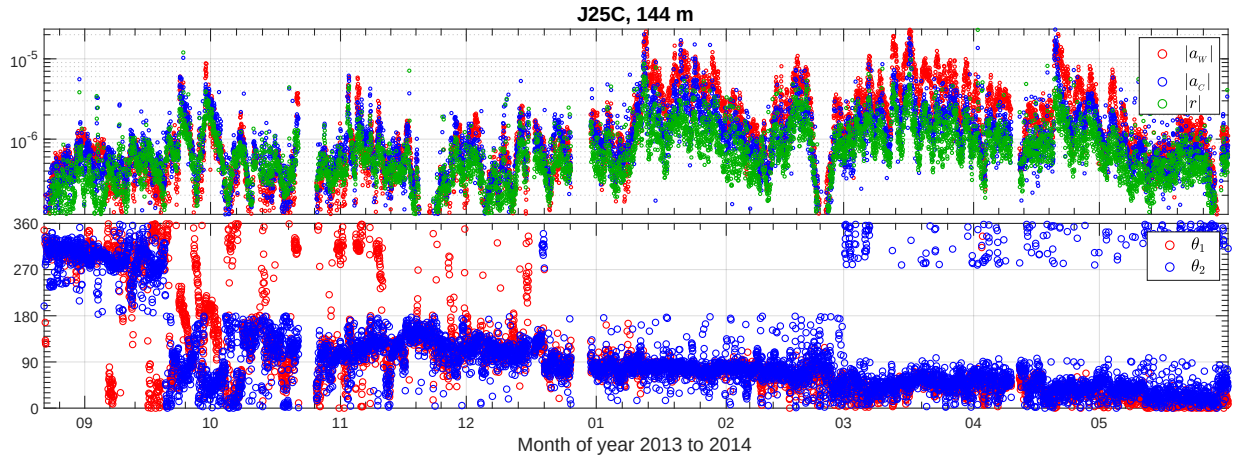
J25C, 144 m
10^{-5}
10^{-6}
$|a_w|$
$|a_c|$
$|r|$
360
270
180
90
0
θ_1
θ_2
09
10
11
12
01
02
03
04
05
Month of year 2013 to 2014

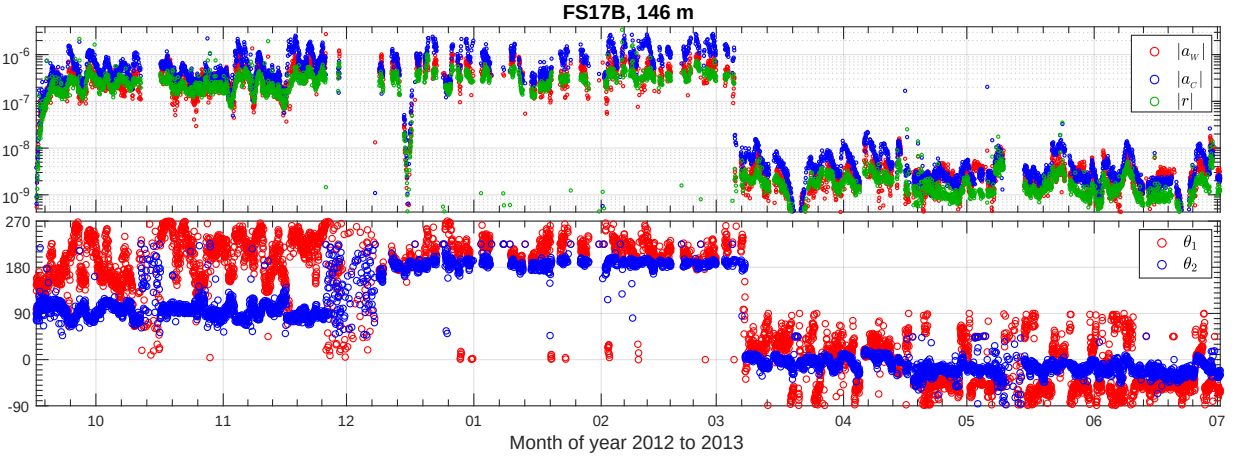
FS17B, 146 m
10^{-6}
10^{-7}
10^{-8}
10^{-9}
$|a_w|$
$|a_c|$
$|r|$
270
180
90
0
-90
θ_1
θ_2
10
11
12
01
02
03
04
05
06
07
Month of year 2012 to 2013

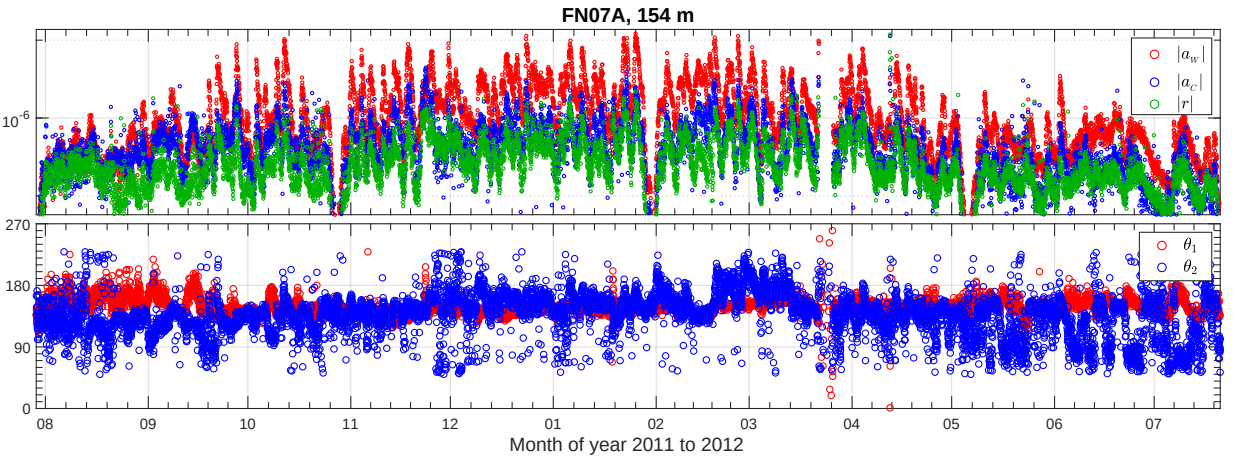
FN07A, 154 m
10^{-6}
$|a_w|$
$|a_c|$
$|r|$
270
180
90
0
θ_1
θ_2
08
09
10
11
12
01
02
03
04
05
06
07
Month of year 2011 to 2012

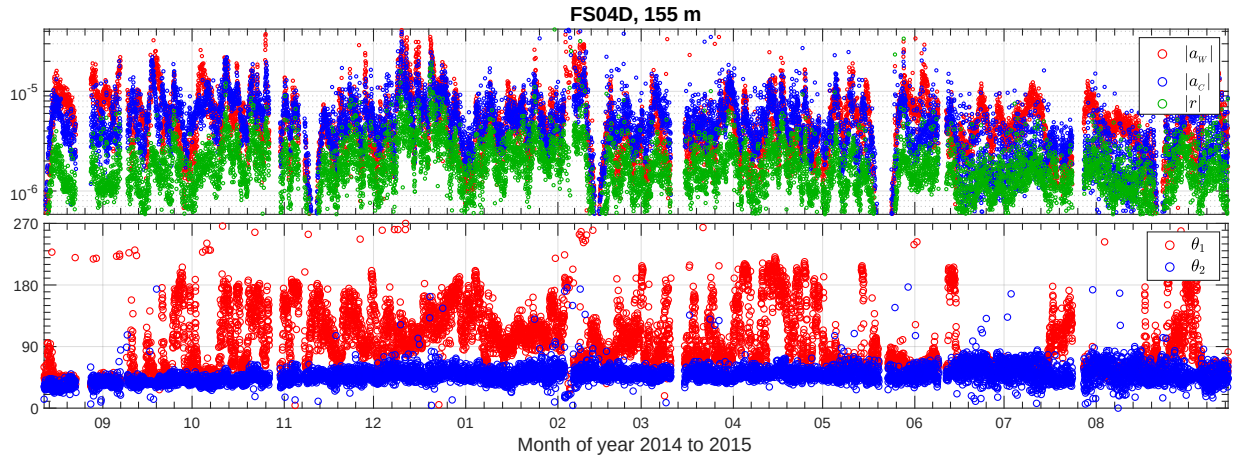
FS04D, 155 m
$|a_w|$
$|a_c|$
$|r|$
10^{-5}
10^{-6}
θ_1
θ_2
270
180
90
0
09
10
11
12
01
02
03
04
05
06
07
08
Month of year 2014 to 2015

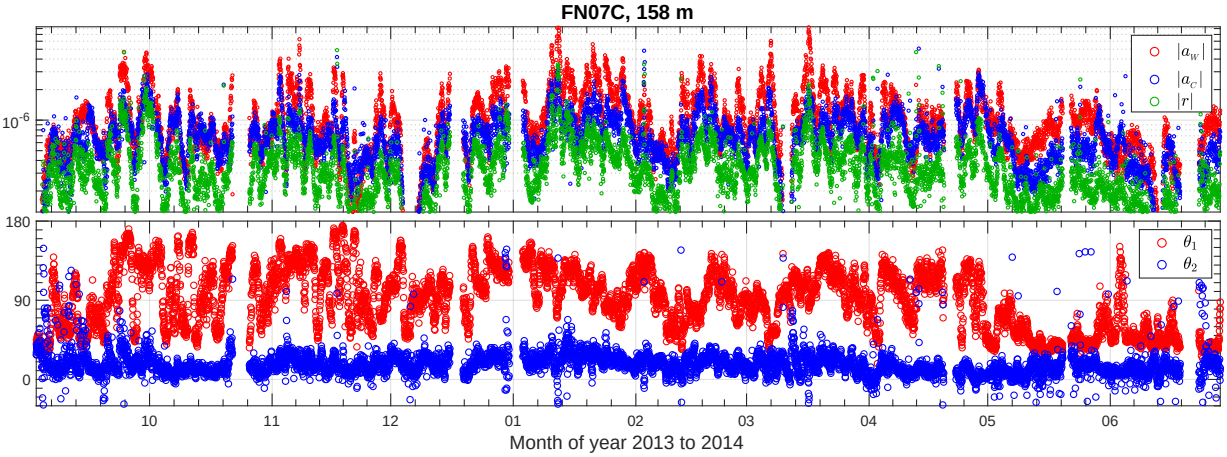
FN07C, 158 m
$|a_w|$
$|a_c|$
$|r|$
10^{-6}
θ_1
θ_2
180
90
0
10
11
12
01
02
03
04
05
06
Month of year 2013 to 2014

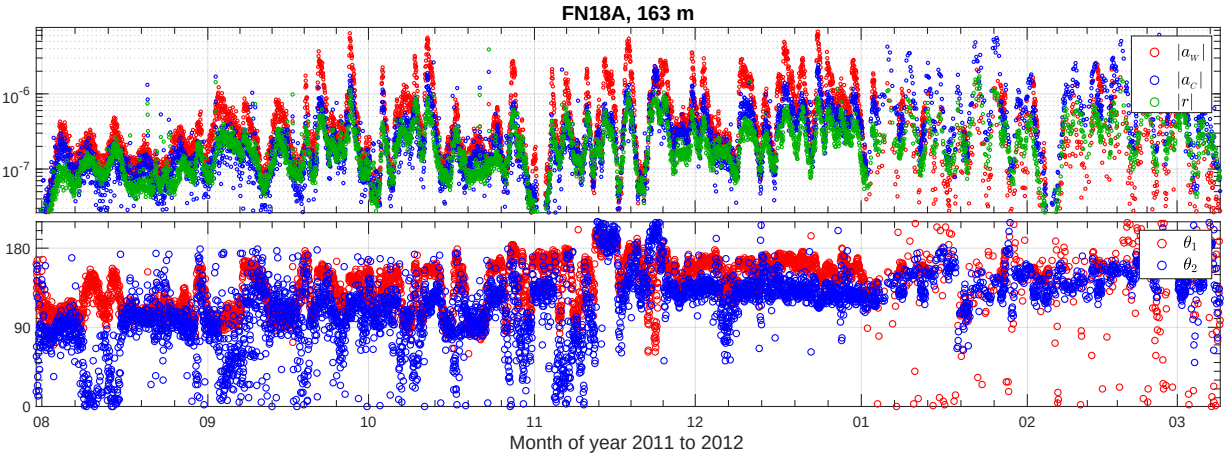
FN18A, 163 m
$|a_w|$
$|a_c|$
$|r|$
10^{-6}
10^{-7}
θ_1
θ_2
180
90
0
08
09
10
11
12
01
02
03
Month of year 2011 to 2012

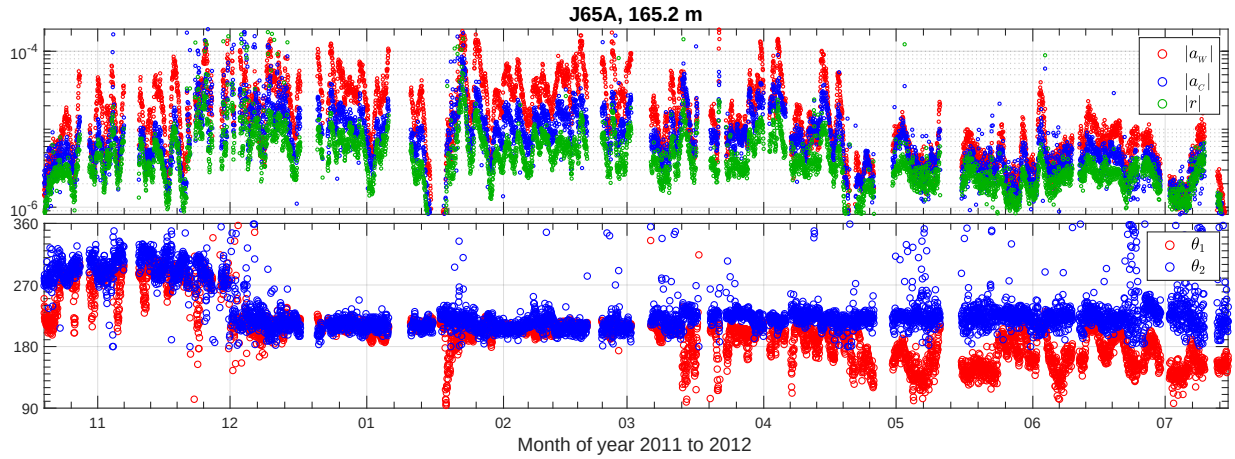
J65A, 165.2 m
10^{-4}
10^{-6}
$|a_w|$
$|a_c|$
$|r|$
360
270
180
90
θ_1
θ_2
11
12
01
02
03
04
05
06
07
Month of year 2011 to 2012

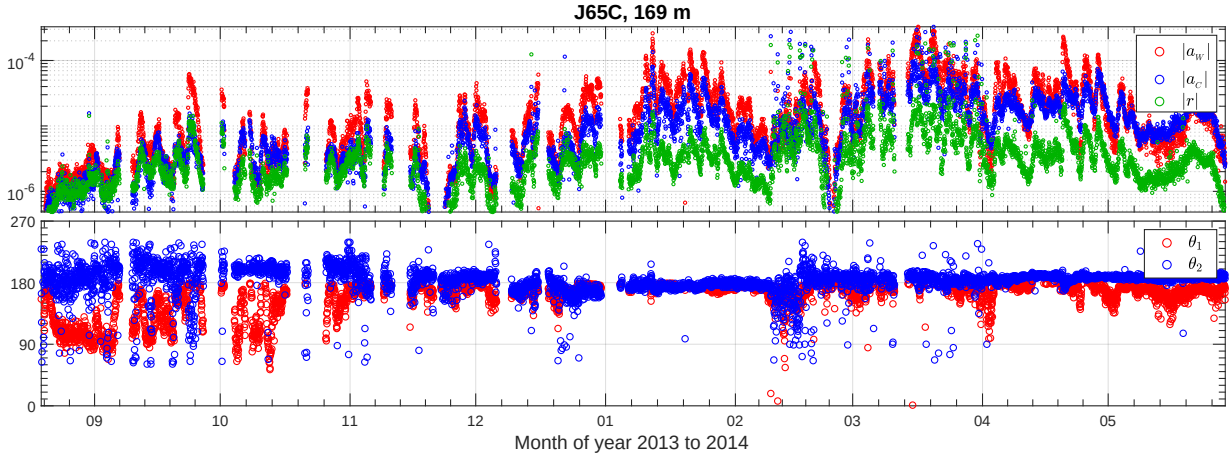
J65C, 169 m
10^{-4}
10^{-6}
$|a_w|$
$|a_c|$
$|r|$
270
180
90
0
θ_1
θ_2
09
10
11
12
01
02
03
04
05
Month of year 2013 to 2014

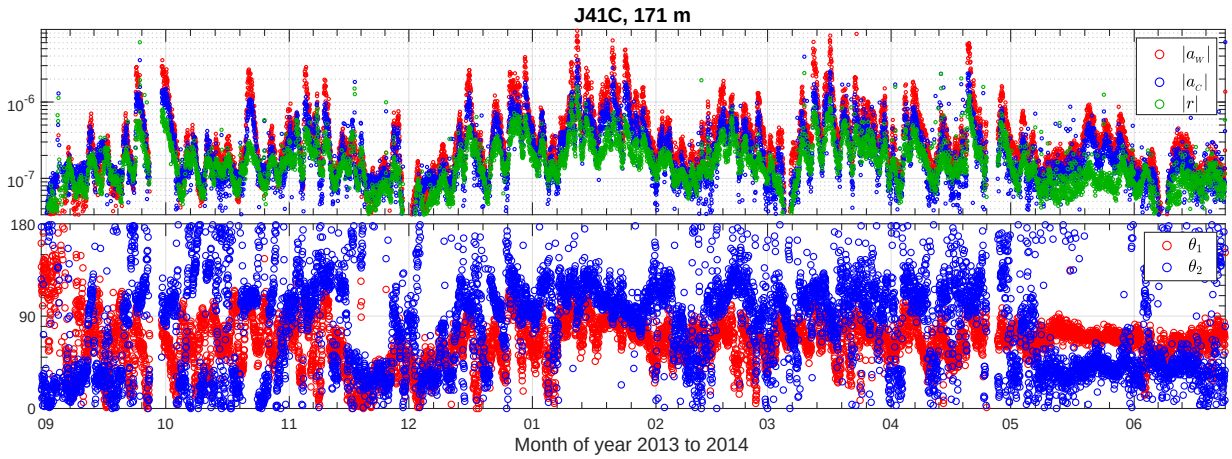
J41C, 171 m
10^{-6}
10^{-7}
$|a_w|$
$|a_c|$
$|r|$
180
90
0
θ_1
θ_2
09
10
11
12
01
02
03
04
05
06
Month of year 2013 to 2014

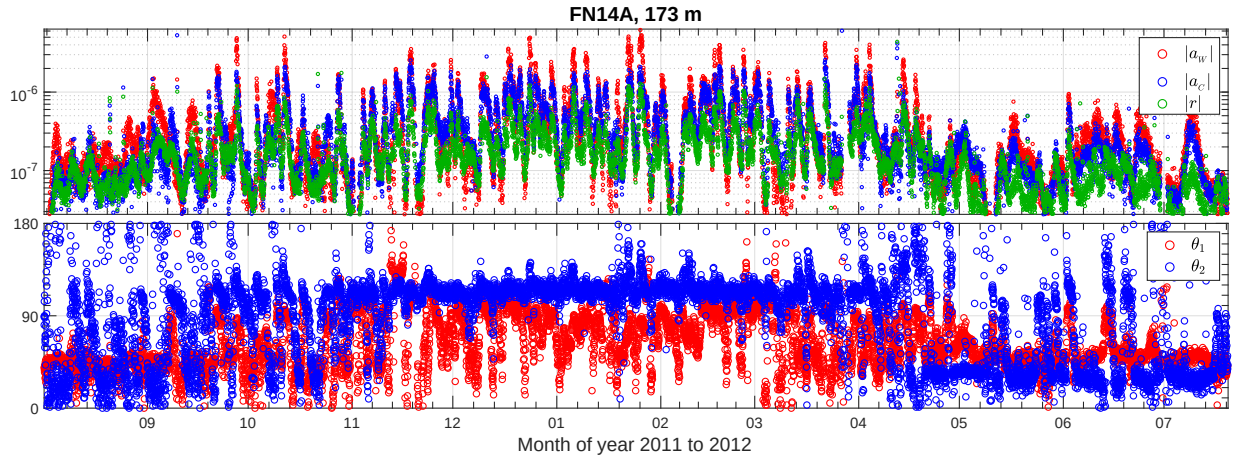
FN14A, 173 m
10^{-6}
10^{-7}
$|a_w|$
$|a_c|$
$|r|$
180
90
0
θ_1
θ_2
09
10
11
12
01
02
03
04
05
06
07
Month of year 2011 to 2012

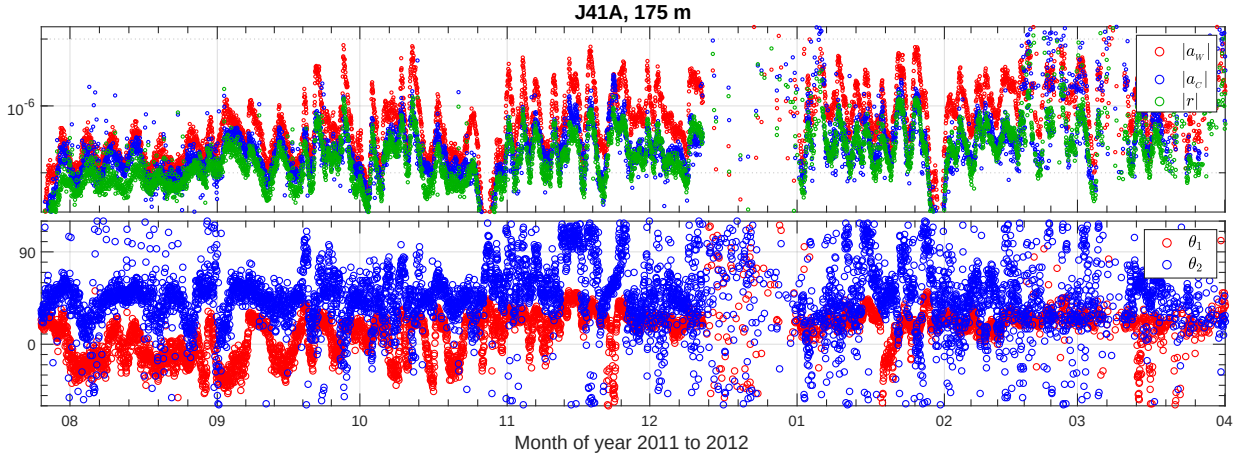
J41A, 175 m
10^{-6}
$|a_w|$
$|a_c|$
$|r|$
90
0
θ_1
θ_2
08
09
10
11
12
01
02
03
04
Month of year 2011 to 2012

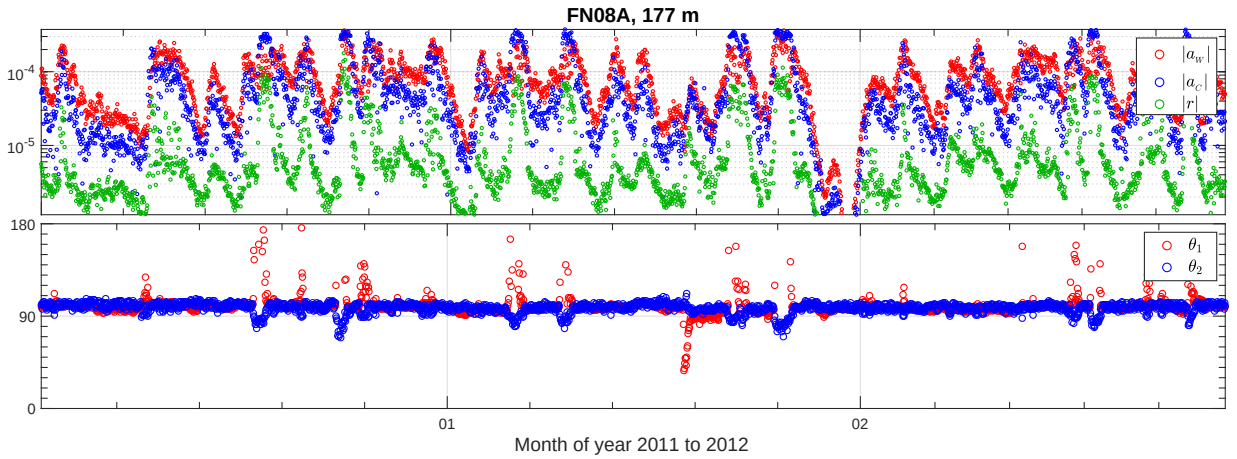
FN08A, 177 m
10^{-4}
10^{-5}
$|a_w|$
$|a_c|$
$|r|$
180
90
0
θ_1
θ_2
01
02
Month of year 2011 to 2012

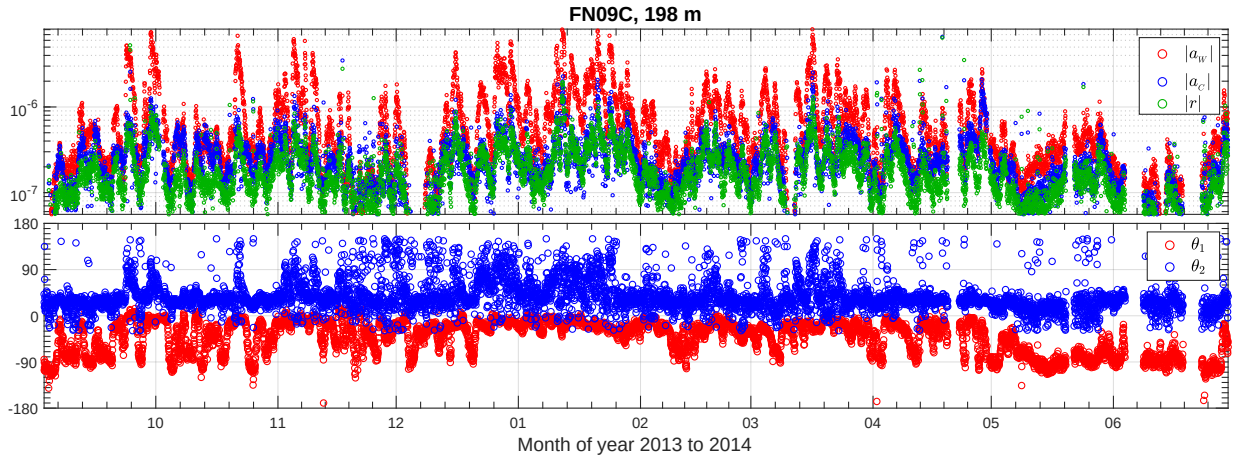
FN09C, 198 m
$|a_w|$
$|a_c|$
$|r|$
10^{-6}
10^{-7}
180
90
0
-90
-180
θ_1
θ_2
10
11
12
01
02
03
04
05
06
Month of year 2013 to 2014

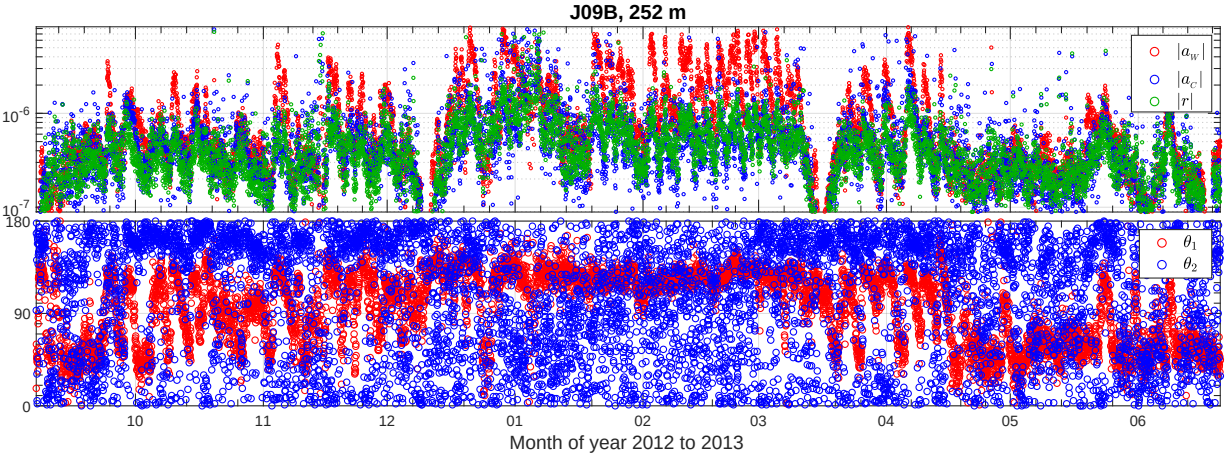
J09B, 252 m
$|a_w|$
$|a_c|$
$|r|$
10^{-6}
10^{-7}
180
90
0
θ_1
θ_2
10
11
12
01
02
03
04
05
06
Month of year 2012 to 2013

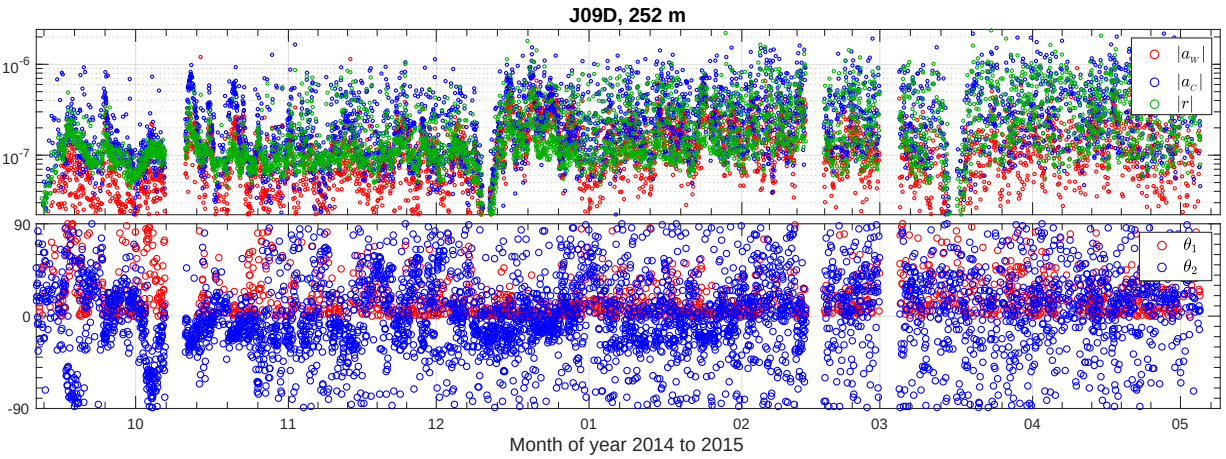
J09D, 252 m
$|a_w|$
$|a_c|$
$|r|$
10^{-6}
10^{-7}
90
0
-90
θ_1
θ_2
10
11
12
01
02
03
04
05
Month of year 2014 to 2015

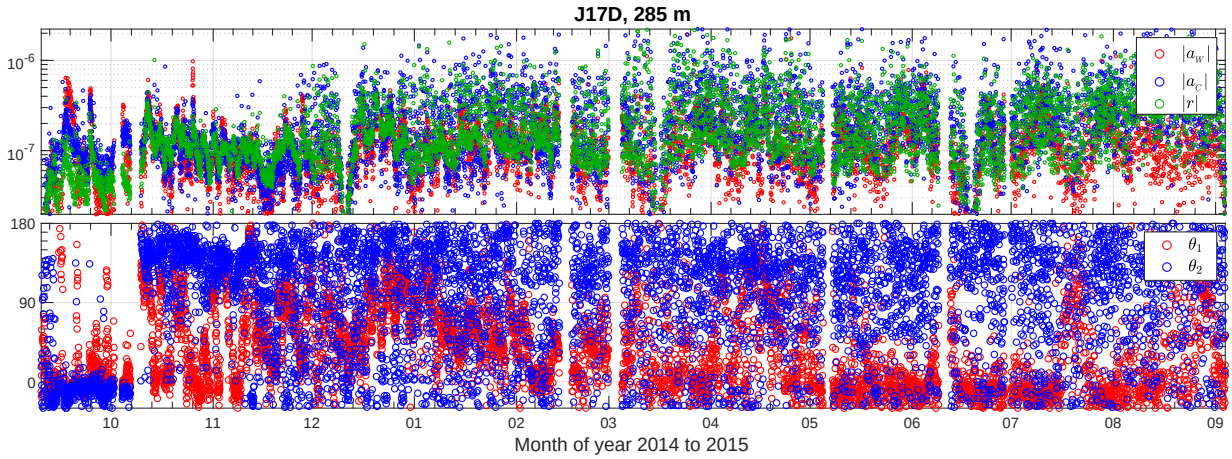

Figure S1. The calculated $|a_W|$, $|a_C|$, $|r|$, θ_1 and θ_2 at all 37 stations.

Figure S2

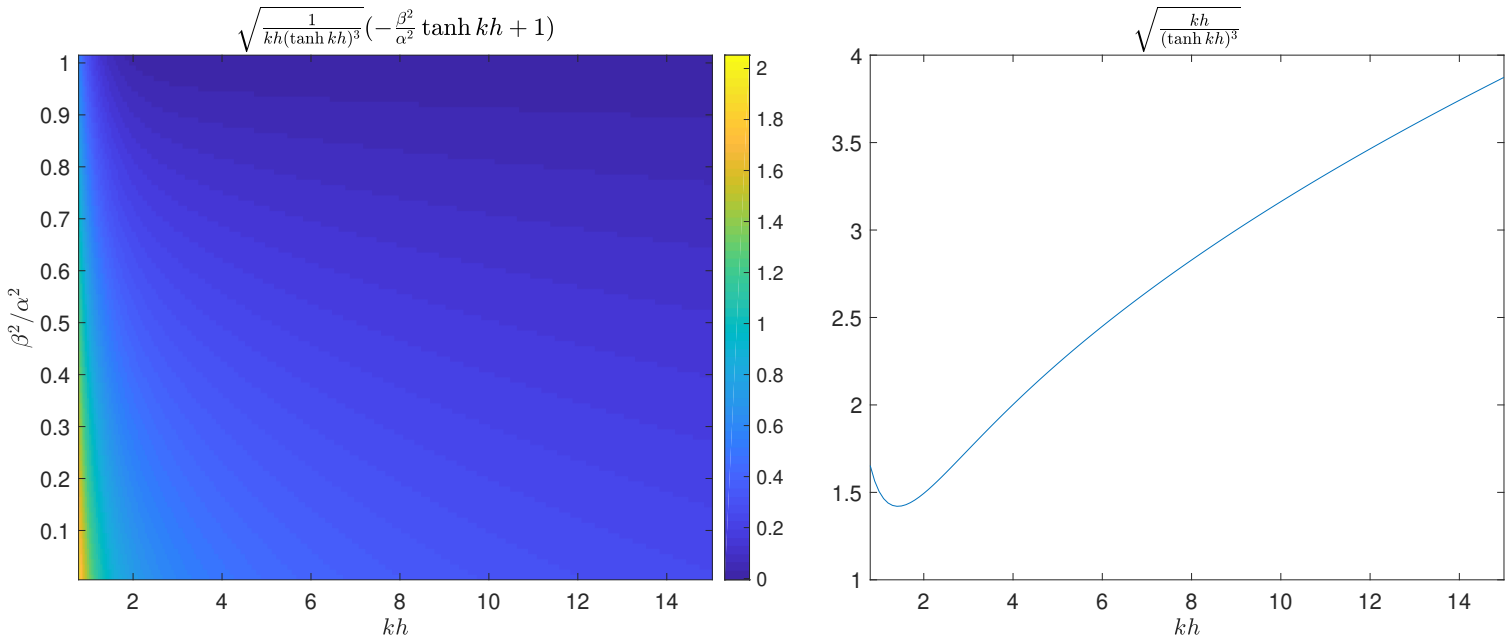

Figure S2. The left and right panels display the kh dependence of K_1^* and K_1^*, respectively. The range of kh extends from 0.8 to 15, corresponding to frequencies between 0.05 and 0.1 Hz, and water depth changes from 50 to 370 m. The results indicate that K_1^* decreases with increasing kh for any β^2/α^2, while K_2^* generally increases. A decrease in K_2^* is observed only at very small values of kh, corresponding to the lowest frequency ($\approx$ 0.05 Hz) and shallowest water ($\approx$ 50 m).

Figure S3

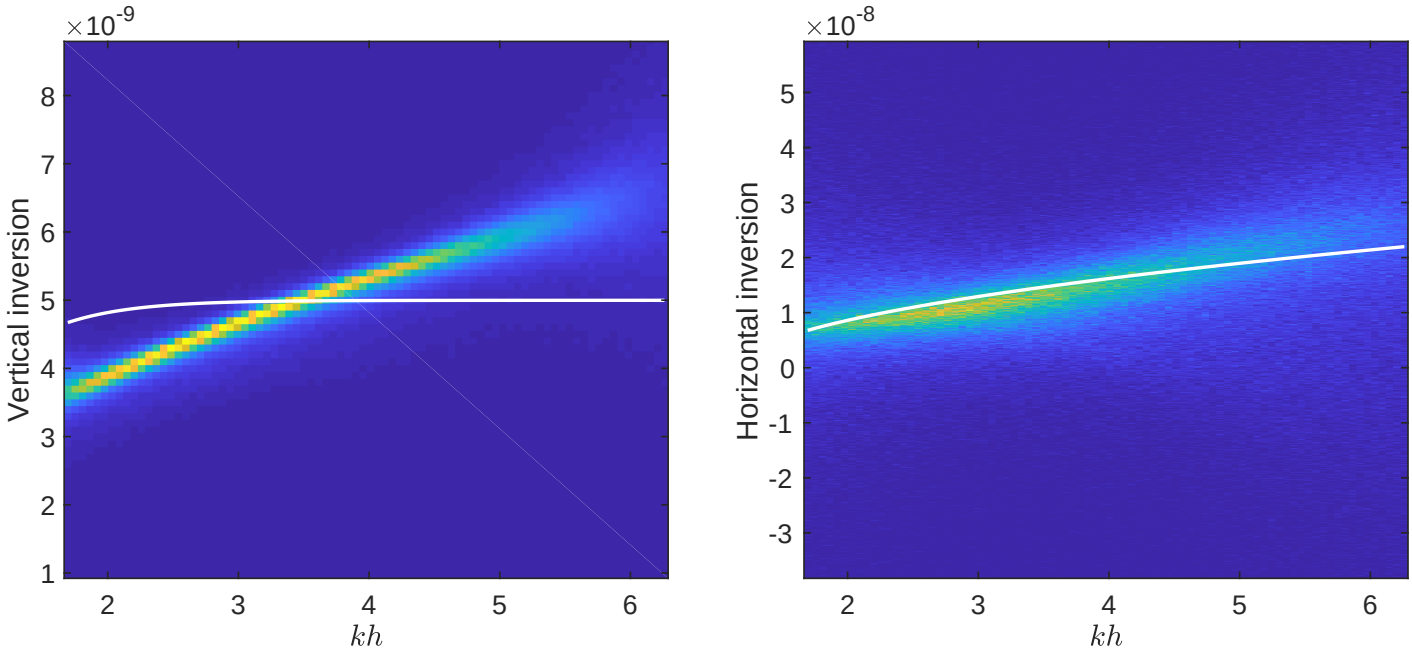

Figure S3. Joint inversion using the horizontal and vertical water wave noise at station FN07A. The optimal inversion parameters are determined to be $\mu = 1.49 \times 10^9$, $\beta^2/\alpha^2 = 0.62$, and $C_3 = 1 \times 10^{-8}$. Using a layered model could potentially improve the inversion results.

Figure S4

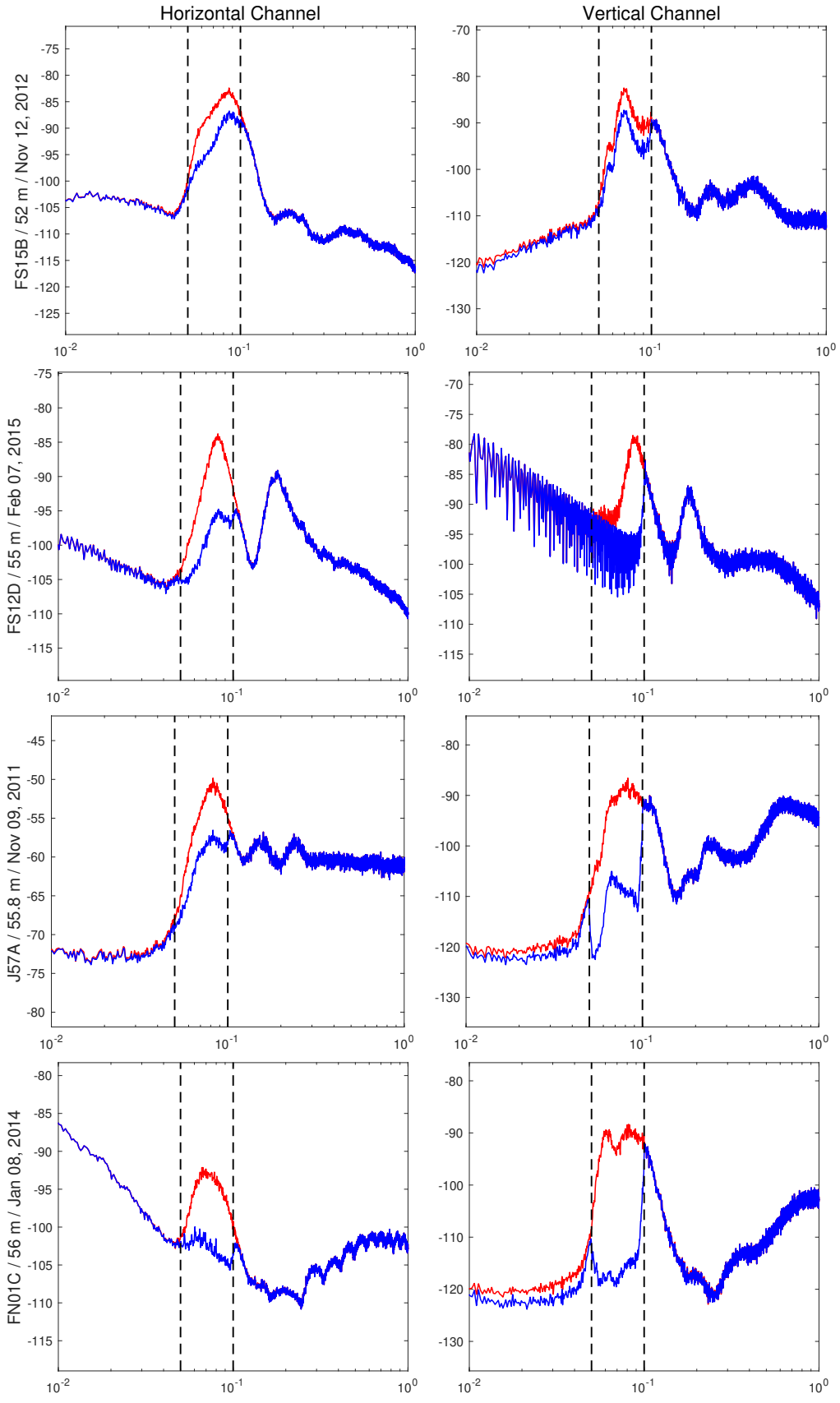
Horizontal Channel
Vertical Channel
FS15B / 52 m / Nov 12, 2012
FS12D / 55 m / Feb 07, 2015
J57A / 55.8 m / Nov 09, 2011
FN01C / 56 m / Jan 08, 2014

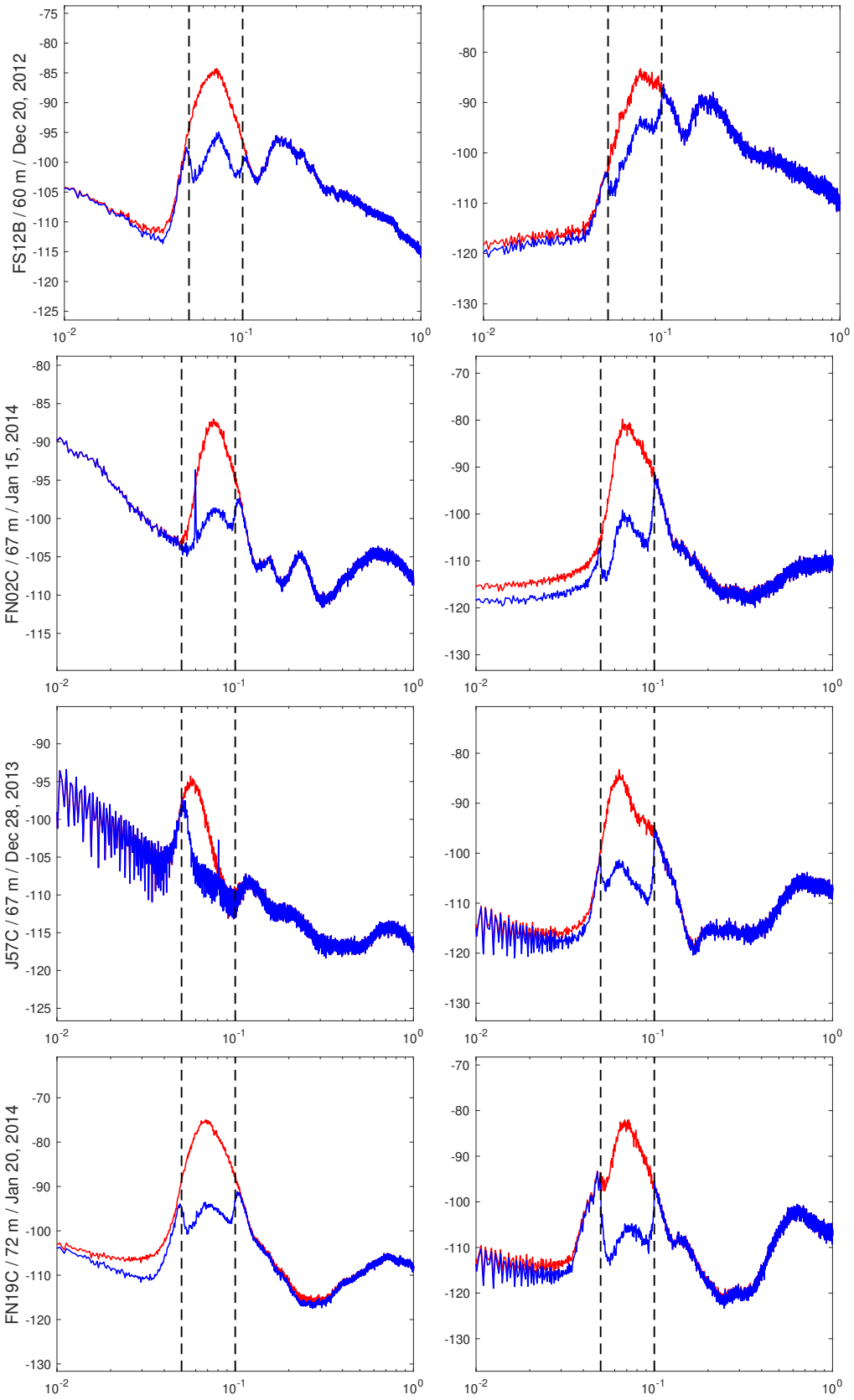
FS12B / 60 m / Dec 20, 2012
FN02C / 67 m / Jan 15, 2014
J57C / 67 m / Dec 28, 2013
FN19C / 72 m / Jan 20, 2014

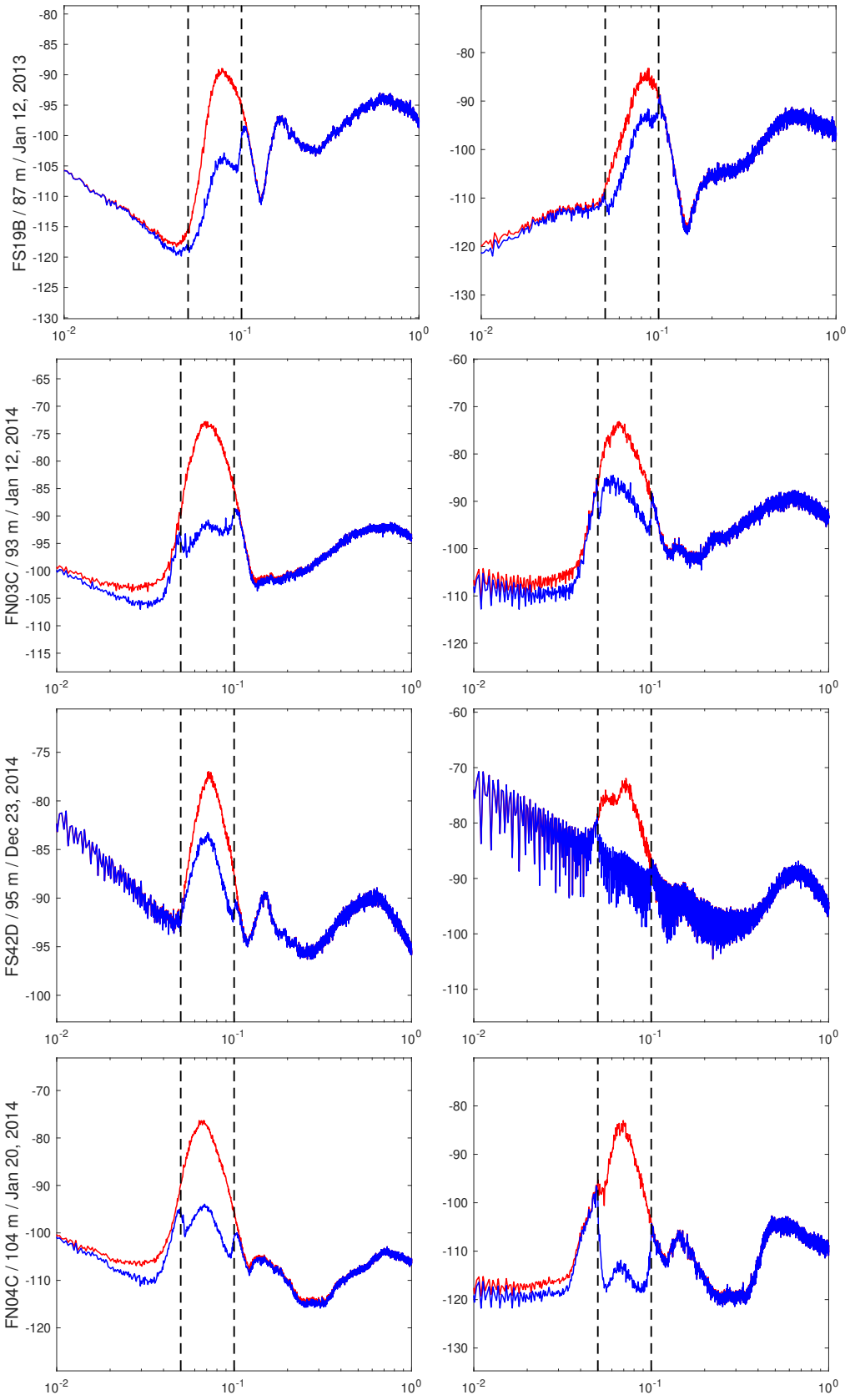
FS19B / 87 m / Jan 12, 2013
FN03C / 93 m / Jan 12, 2014
FS42D / 95 m / Dec 23, 2014
FN04C / 104 m / Jan 20, 2014

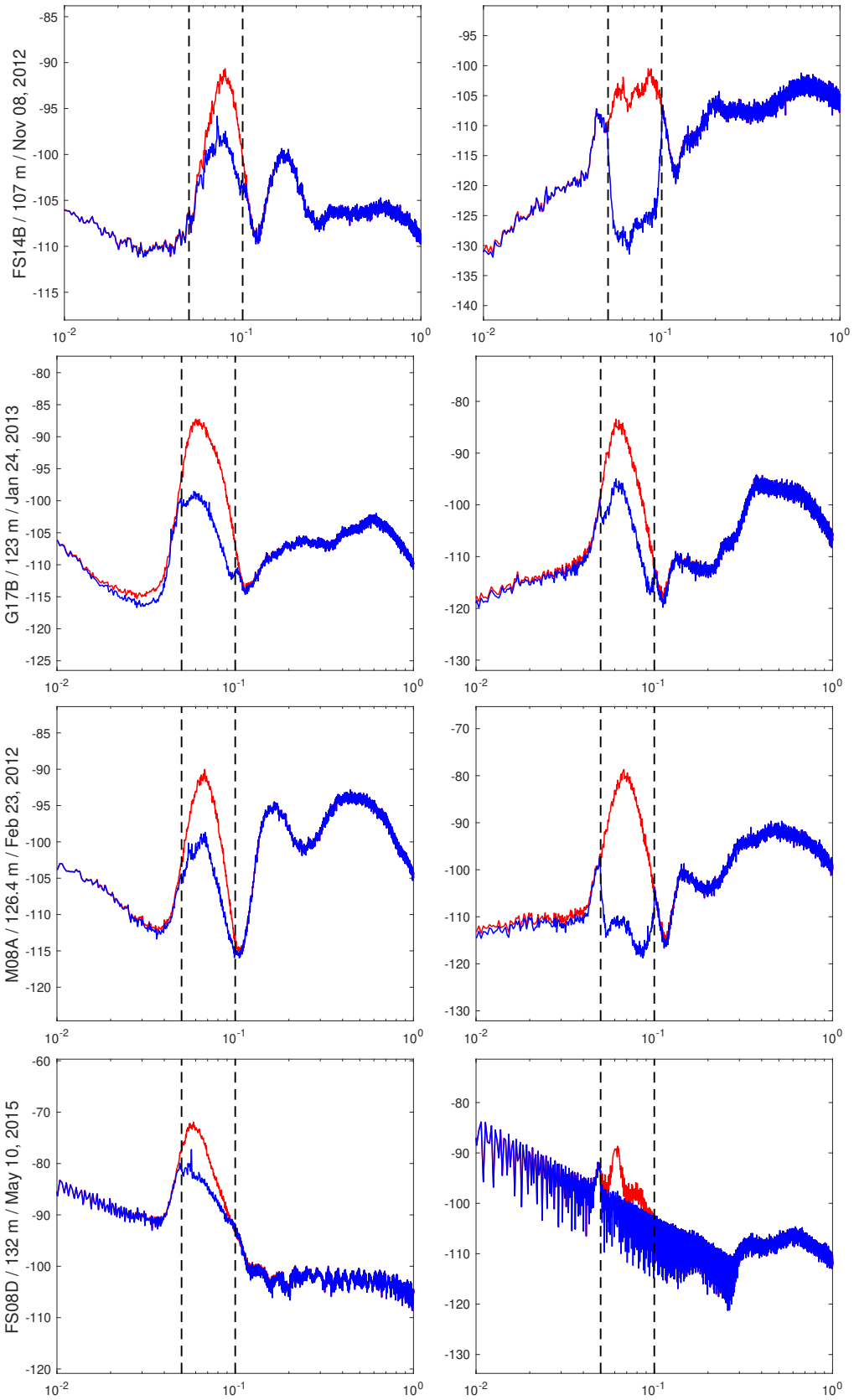
FS14B / 107 m / Nov 08, 2012
G17B / 123 m / Jan 24, 2013
M08A / 126.4 m / Feb 23, 2012
FS08D / 132 m / May 10, 2015

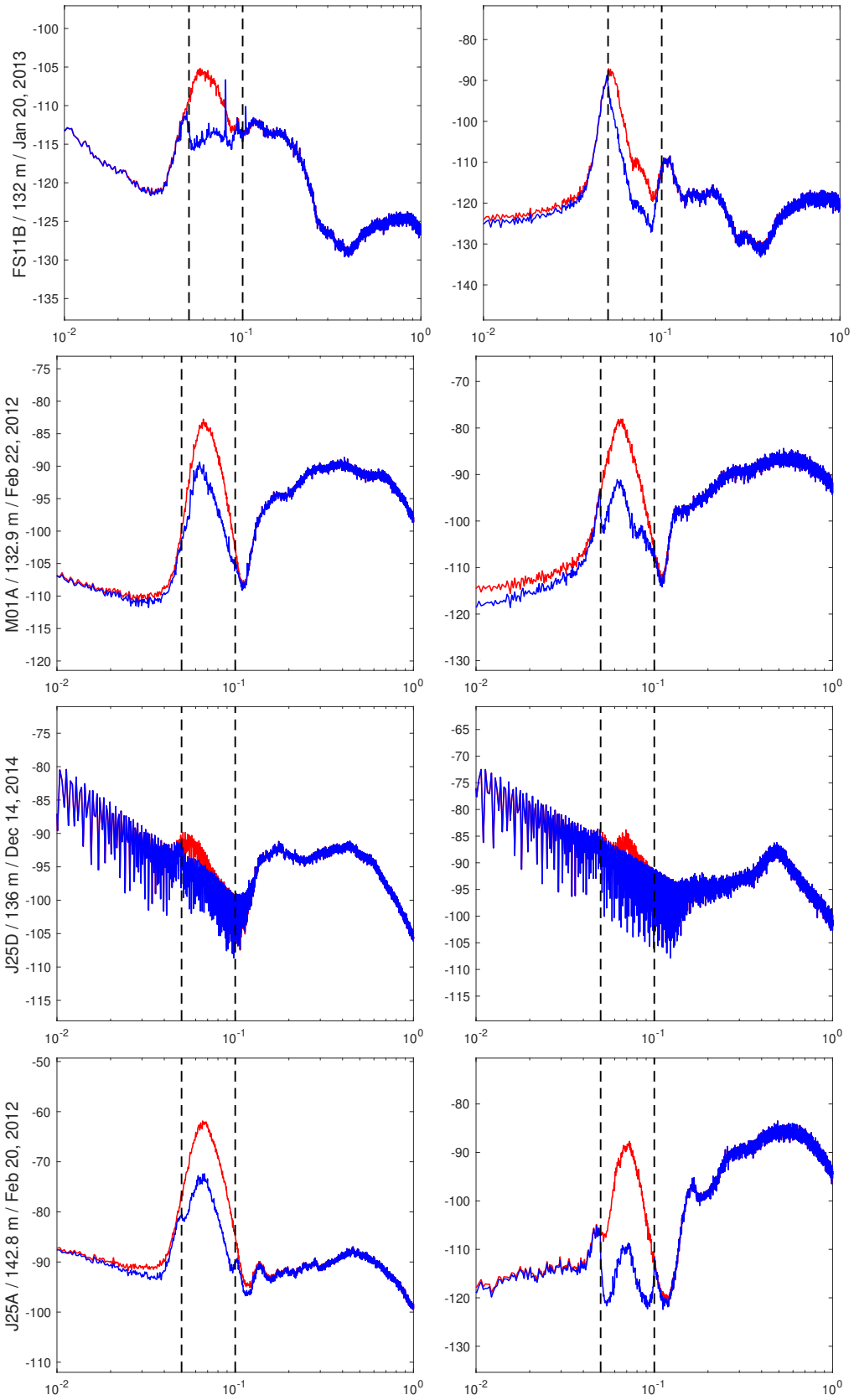
FS11B / 132 m / Jan 20, 2013
M01A / 132.9 m / Feb 22, 2012
J25D / 136 m / Dec 14, 2014
J25A / 142.8 m / Feb 20, 2012

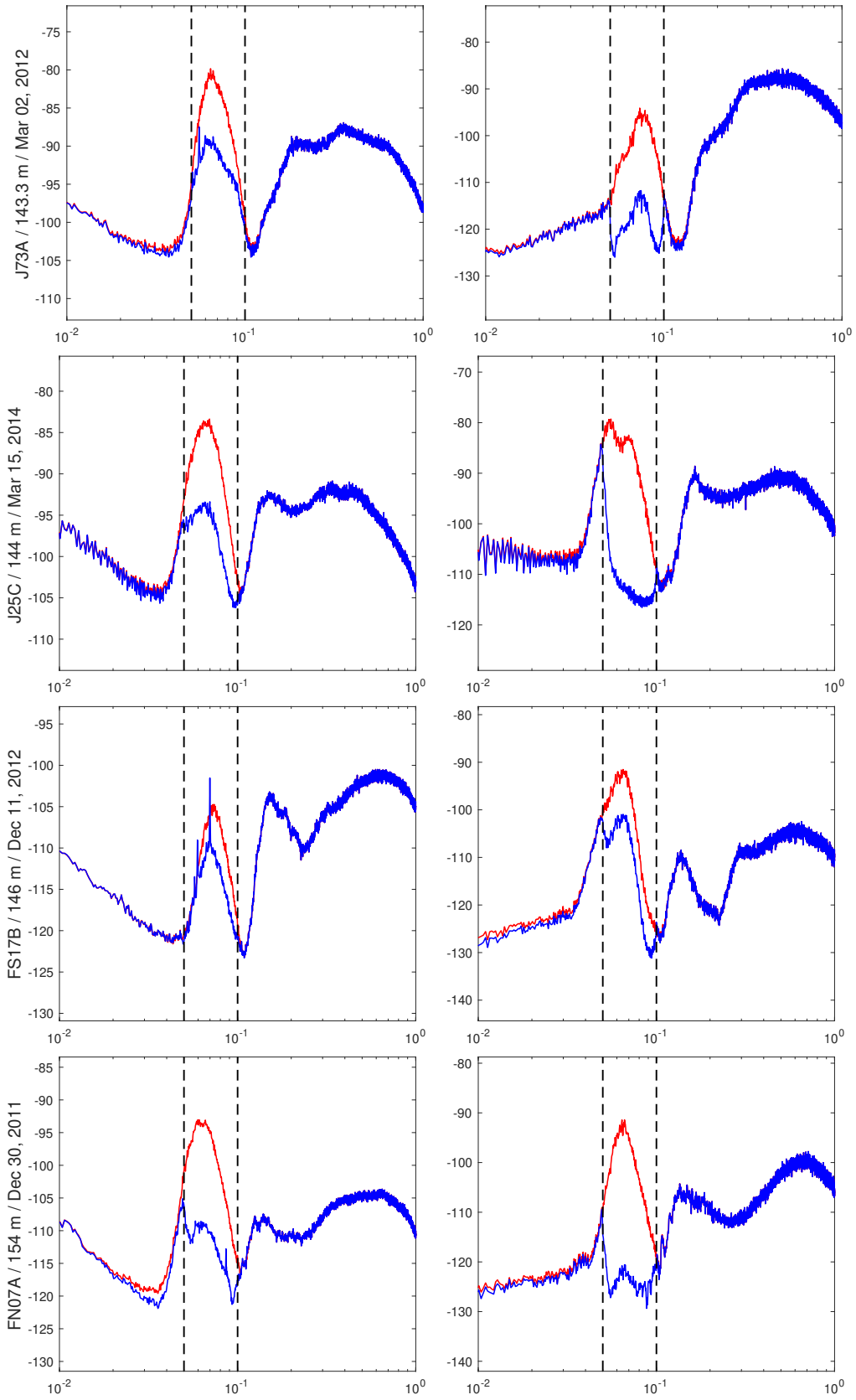
J73A / 143.3 m / Mar 02, 2012
J25C / 144 m / Mar 15, 2014
FS17B / 146 m / Dec 11, 2012
FN07A / 154 m / Dec 30, 2011

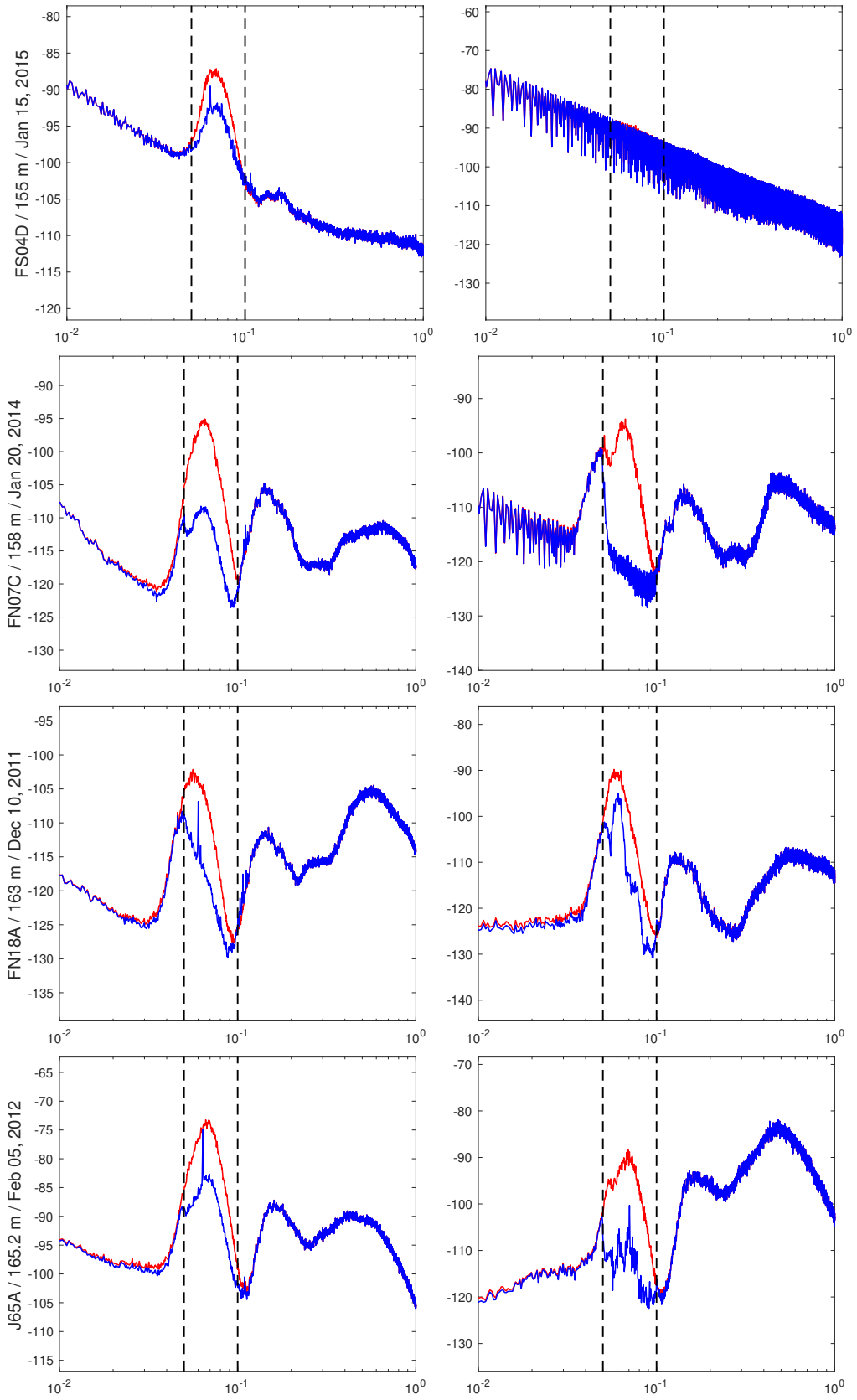
FS04D / 155 m / Jan 15, 2015
FN07C / 158 m / Jan 20, 2014
FN18A / 163 m / Dec 10, 2011
J65A / 165.2 m / Feb 05, 2012

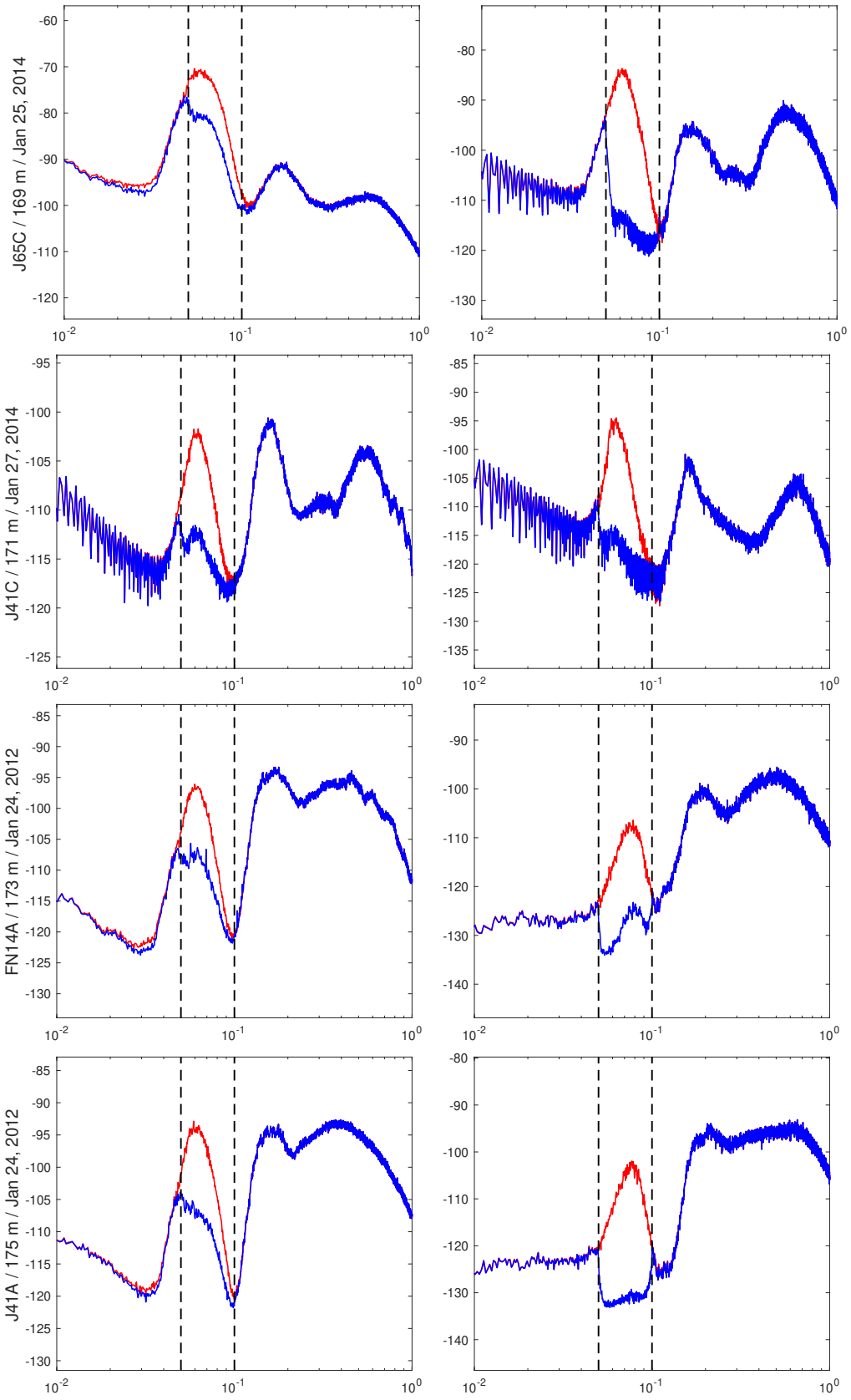
J65C / 169 m / Jan 25, 2014
J41C / 171 m / Jan 27, 2014
FN14A / 173 m / Jan 24, 2012
J41A / 175 m / Jan 24, 2012

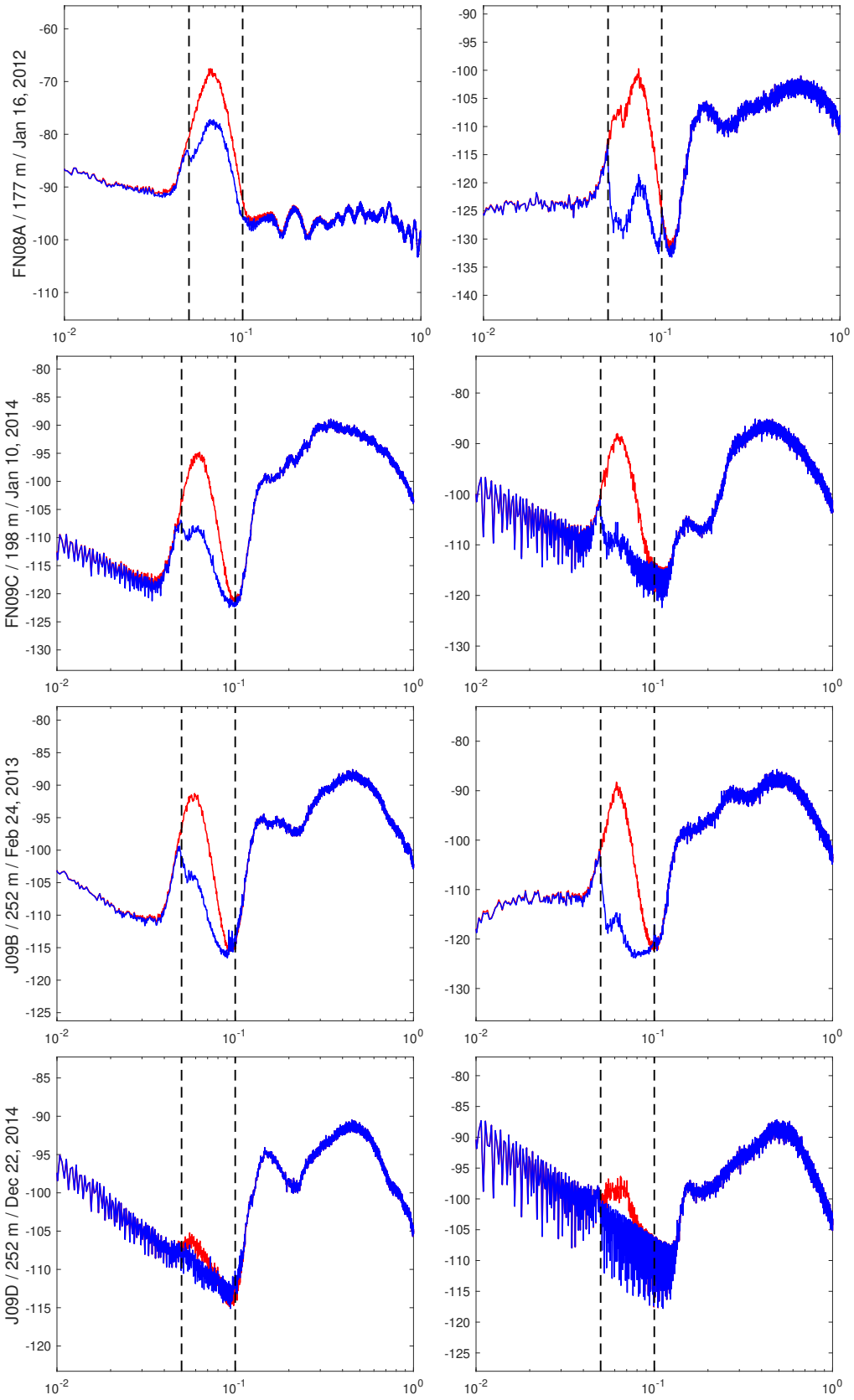
FN08A / 177 m / Jan 16, 2012
FN09C / 198 m / Jan 10, 2014
J09B / 252 m / Feb 24, 2013
J09D / 252 m / Dec 22, 2014

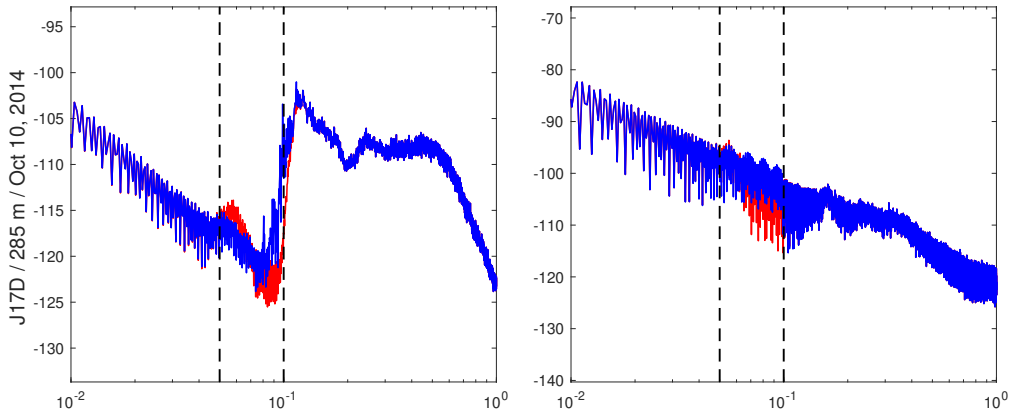

Figure S4. Average Power Spectral Densities (PSDs) for days with strong waves at all 37 stations, both before (red) and after (blue) noise removal. The left and right panels show the horizontal and vertical channels, respectively.

Figure S5

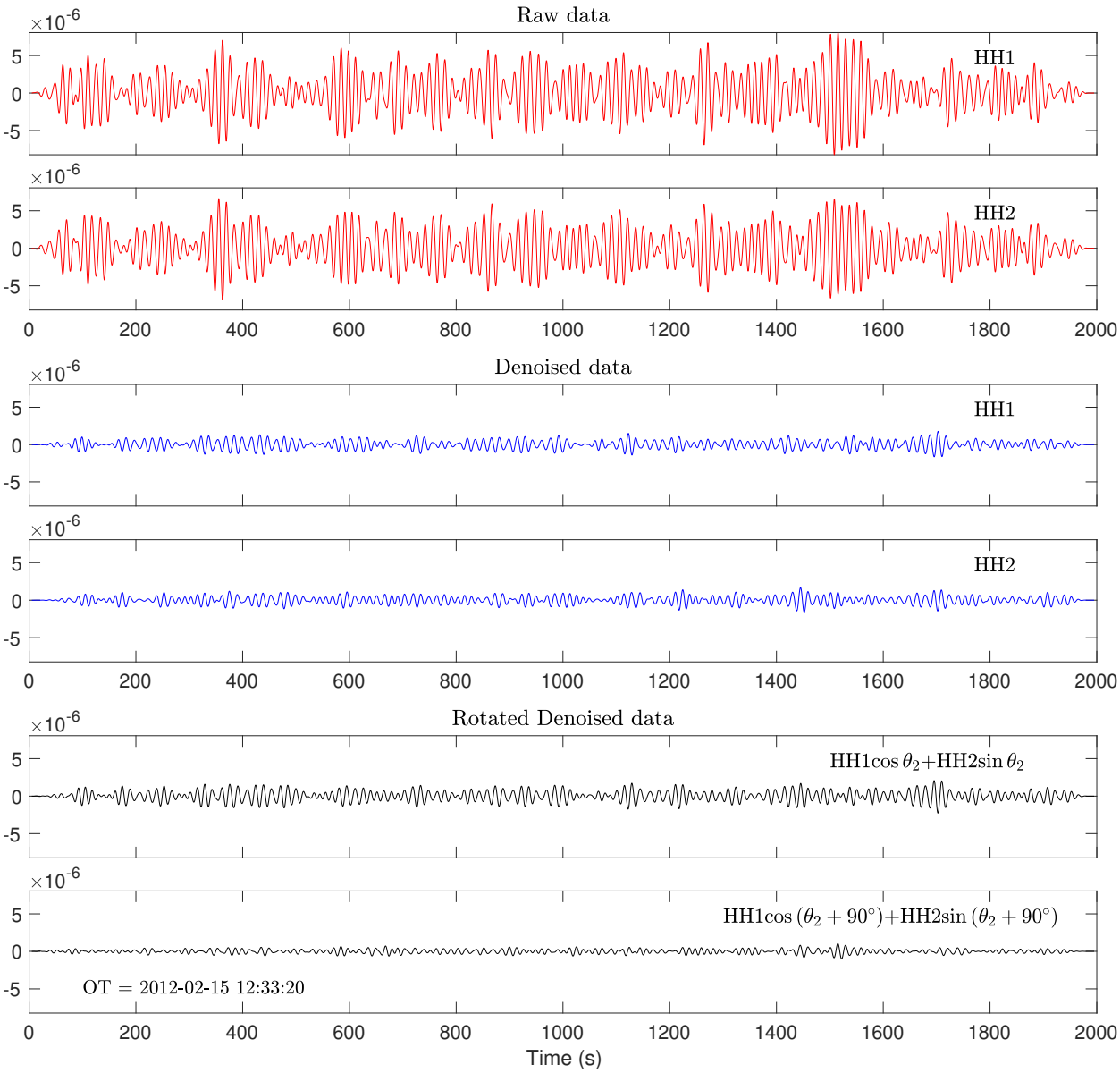

Figure S5. An example to demonstrate the removal of wave noise a_W and other noise a_C at station FN07A. The raw data from FN07A are initially filtered between 0.05 – 0.1 Hz (red). The wave noise a_W is eliminated using HPTF predictions to obtain the denoised data (blue). Subsequently, the data are rotated to align with and perpendicular to θ_2 (black). For this example, $\theta_1 = 49°$, $\theta_2 = 47°$.